

## Evaluating the antibacterial efficacy of a silver nanocomposite surface coating against nosocomial pathogens as an antibiofilm strategy to prevent hospital infections

James Butler, Sian Morgan, Lewis Jones, Mathew Upton & Alexandros Besinis

To cite this article: James Butler, Sian Morgan, Lewis Jones, Mathew Upton & Alexandros Besinis (25 Jul 2024): Evaluating the antibacterial efficacy of a silver nanocomposite surface coating against nosocomial pathogens as an antibiofilm strategy to prevent hospital infections, *Nanotoxicology*, DOI: [10.1080/17435390.2024.2379809](https://doi.org/10.1080/17435390.2024.2379809)

To link to this article: <https://doi.org/10.1080/17435390.2024.2379809>



© 2024 The Author(s). Published by Informa UK Limited, trading as Taylor & Francis Group.



[View supplementary material](#)



Published online: 25 Jul 2024.



[Submit your article to this journal](#)



[View related articles](#)



[View Crossmark data](#)

# Evaluating the antibacterial efficacy of a silver nanocomposite surface coating against nosocomial pathogens as an antibiofilm strategy to prevent hospital infections

James Butler<sup>a\*</sup>, Sian Morgan<sup>a</sup>, Lewis Jones<sup>b</sup>, Mathew Upton<sup>c</sup> and Alexandros Besinis<sup>a,d</sup>

<sup>a</sup>School of Engineering, Computing and Mathematics, Faculty of Science and Engineering, University of Plymouth, Plymouth, United Kingdom; <sup>b</sup>Clinical Microbiology, University Hospitals Plymouth NHS Trust, Plymouth, United Kingdom; <sup>c</sup>School of Biomedical Sciences, Faculty of Health, University of Plymouth, Plymouth, United Kingdom; <sup>d</sup>Peninsula Dental School, Faculty of Health, University of Plymouth, Plymouth, United Kingdom

## ABSTRACT

Antimicrobial nanocoatings may be a means of preventing nosocomial infections, which account for significant morbidity and mortality. The role of hospital sink traps in these infections is also increasingly appreciated. We describe the preparation, material characterization and antibacterial activity of a pipe cement-based silver nanocoating applied to unplasticized polyvinyl chloride, a material widely used in wastewater plumbing. Three-dimensional surface topography imaging and scanning electron microscopy showed increased roughness in all surface finishes versus control, with grinding producing the roughest surfaces. Silver stability within nanocoatings was >99.89% in deionized water and bacteriological media seeded with bacteria. The nanocoating exhibited potent antibiofilm (99.82–100% inhibition) and antiplanktonic (99.59–99.99% killing) activity against three representative bacterial species and a microbial community recovered from hospital sink traps. Hospital sink trap microbiota were characterized by sequencing the 16S rRNA gene, revealing the presence of opportunistic pathogens from genera including *Pseudomonas*, *Enterobacter* and *Clostridioides*. In a benchtop model sink trap system, nanocoating antibiofilm activity against this community remained significant after 11 days but waned following 25 days. Silver nanocoated disks in real-world sink traps in two university buildings had a limited antibiofilm effect, even though *in vitro* experiments using microbial communities recovered from the same traps demonstrated that the nanocoating was effective, reducing biofilm formation by >99.6% and killing >98% of planktonic bacteria. We propose that conditioning films forming in the complex conditions of real-world sink traps negatively impact nanocoating performance, which may have wider relevance to development of antimicrobial nanocoatings that are not tested in the real-world.

## ARTICLE HISTORY

Received 26 March 2024  
Revised 4 July 2024  
Accepted 5 July 2024



## KEYWORDS


Antimicrobial; nanocoating;  
16S; wastewater; biofilm

## 1. Introduction

Significant morbidity and mortality in healthcare can be attributed to nosocomial infections, also known as healthcare- or hospital-associated infections (Koch et al. 2015; Cassini et al. 2016; National Institute for Health and Care Excellence 2016). Besides human-to-human transmission, these infections may result from invasive medical devices such as dental implants, indwelling catheters, mechanical heart valves, contact and droplet transmission

involving surfaces, or by airborne transmission of droplets and bioaerosols (Darouiche 2001). Treating bacterial infections with antimicrobial products, including antibiotics, is associated with the emerging major threat of antimicrobial resistance, the result of selection for mutations allowing bacteria to evade drugs intended to kill them or inhibit their growth. Infections caused by antibiotic resistant bacteria killed 1.27 million people in 2019 (Murray et al. 2022) and antimicrobial resistance has been exacerbated by the COVID-19 pandemic (CDC 2022).

**CONTACT** Alexandros Besinis  alexander.besinis@plymouth.ac.uk  School of Engineering, Computing and Mathematics, Faculty of Science and Engineering, University of Plymouth, Plymouth PL4 8AA, United Kingdom

 Supplemental data for this article can be accessed online at <https://doi.org/10.1080/17435390.2024.2379809>.

\*Present address: Department of Clinical and Biomedical Sciences, Exeter Medical School, Faculty of Health and Life Sciences, University of Exeter, Exeter EX1 2LU, United Kingdom.

© 2024 The Author(s). Published by Informa UK Limited, trading as Taylor & Francis Group.

This is an Open Access article distributed under the terms of the Creative Commons Attribution-NonCommercial-NoDerivatives License (<http://creativecommons.org/licenses/by-nc-nd/4.0/>), which permits non-commercial re-use, distribution, and reproduction in any medium, provided the original work is properly cited, and is not altered, transformed, or built upon in any way. The terms on which this article has been published allow the posting of the Accepted Manuscript in a repository by the author(s) or with their consent.

If growth in resistant infections continues at current rates, by 2050 they are expected to kill 10 million people globally per year (O'Neill 2016). There were 834,000 nosocomial infections and 28,500 resulting patient deaths reported in the period 2016–2017 across all NHS hospitals in England (Guest et al. 2020), with the cost of these potentially preventable infections calculated at between £1 billion (Mackley, Baker, and Bate 2018) and £2.7 billion (Guest et al. 2020).

Sink traps (with configurations including U-bends, P-traps and bottle traps) connect sink drains to waste in both domestic and commercial wastewater plumbing systems. They are designed to trap water during use to create a seal, preventing flow of gases from the sewer to the sink and surrounding environment. In hospitals, most wards and individual patient rooms contain sinks to encourage good hand hygiene and achieve infection prevention and control (Rashid 2006). However, sink traps can become heavily colonized with opportunistically pathogenic bacteria such as *Pseudomonas aeruginosa*, *Acinetobacter baumannii*, *Klebsiella* spp., *Citrobacter* spp., *Enterobacter* spp. and *Serratia marcescens* (Lowe et al. 2012; Landelle et al. 2013; Loveday et al. 2014; Regev-Yochay et al. 2018; Volling et al. 2020; Franco et al. 2020; Jamal et al. 2020; De Geyter et al. 2021; Nurjadi et al. 2021; Kehl et al. 2022), and act as a reservoir for pathogens causing nosocomial infections (Volling et al. 2020; Quick et al. 2014; Walker et al. 2014; Gormley et al. 2017; Halstead et al. 2021). While augmented environmental cleaning measures have been shown to reduce nosocomial infection rates (Mitchell et al. 2019), bacteria are able to persist long-term in wastewater plumbing systems through biofilm formation (Vickery et al. 2012; Burgos-Garay et al. 2021). Biofilm development is the process where bacteria attach to surfaces, orchestrate their communal activities via quorum sensing, and produce extracellular polymeric substances to bind and protect cells from disinfection (Flemming et al. 2016). When a sink is used, bacteria residing in the sink traps can also be dispersed into the plumbing pipework and escape encapsulated in droplets and aerosols (Hota et al. 2009; Kotay et al. 2017; Hajar et al. 2019; Yui et al. 2019), moving on airflows within wastewater plumbing systems between different floors of the same building (Gormley et al. 2017).

In order to combat antimicrobial resistance, there is a need to reduce excessive use of antibiotics and conduct research to discover new antibiotics. It is also important that parallel actions to improve water, sanitation and hygiene and infection prevention and

control are taken (Global and Public Health Group (Emergency Preparedness and Health Protection Policy Directorate) 2019). To widen infection prevention and control measures outside the more routine and traditional approaches such as hand hygiene, use of personal protective equipment, respiratory and cough hygiene and waste management, a range of novel antibacterial strategies are being sought, including ways to reduce the bacterial impact on wastewater plumbing systems. A major breakthrough would be the inhibition of biofilm formation, which would interrupt the persistence of potentially pathogenic bacteria by preventing the formation of a mature community before it becomes more difficult to eradicate (Singh et al. 2017). Certain metal or metal oxide nanoparticles (silver, zinc, copper, titanium dioxide), as well as composite nanomaterials (e.g., Cd-Se quantum dots) are known to have strong antimicrobial properties (Allaker 2010) and have been used for infection prevention and control (Parani et al. 2016). The application of such nanomaterials with intrinsic antimicrobial properties has previously been investigated to inhibit biofilm development on surfaces (Qayyum and Khan 2016; Butler et al. 2023). Previous studies have demonstrated that silver (Ag) nanoparticles (NPs) applied directly to human dentin in the form of nanocoatings resulted in strong bactericidal activity and inhibited bacterial adhesion far better than traditional clinical antiseptics (Besinis et al., 2014a). Similar Ag nanocoatings were also found to have very strong antibacterial and antibiofilm activity in medical implant applications (Besinis et al. 2017) and inhibit fungal growth *in vitro* when applied to silicone maxillofacial prostheses (Meran et al. 2018).

The hypothesis of this study was that developing a novel Ag nanocomposite coating could reduce bacterial biofilm formation on polymer pipe surfaces. The rationale of the study was based on previous work (Besinis et al., 2014a; Besinis et al. 2017; Meran et al. 2018; Besinis et al., 2014b) where application of antimicrobial nanomaterials to various substrates showed strong antiplanktonic effects and biofilm inhibition. The first objective was to characterize the nanocoating under investigation and confirm its stability. The second objective was to test the antibacterial efficacy of the applied nanocoating *in vitro* against certain pathogens known to cause nosocomial infections: *Pseudomonas aeruginosa*, *Enterococcus faecalis* and *Acinetobacter baumannii*. The real-world performance of the nanocoating was then evaluated under controlled laboratory conditions using a benchtop sink trap model system to test its efficacy against a bacterial community derived from hospital

sinks. Finally, the antibiofilm activity was also investigated *in situ* against sink trap pathogenic communities in a real-world environment that involved sink traps in workplace toilets.

## 2. Methods and materials

The broad experimental design is summarized by a schematic as shown in Figure 1.

### 2.1. Disk and nanocoating preparation

Round disks with a diameter of 15 mm and thickness of 1 mm were waterjet cut (Waterjet Profiles Ltd., Plymouth, UK) from an unplasticized polyvinyl chloride (uPVC) sheet (Pure Plastics Ltd., Bristol, UK). The preparation of the Ag nanosolutions was performed based on the method previously described by Besinis et al. (2014a). The Ag NPs used were identical to those previously characterized in detail by Besinis et al. (2014b). In this study, Ag nanopowder with a particle size less than 100 nm (Sigma-Aldrich, MO, USA) was mixed with acetone to a concentration of 20 g L<sup>-1</sup> (i.e., two times the final intended Ag concentration), vortexed for 30 s and sonicated (35 kHz, Fisherbrand FB 11010, Germany) in a glass vial for 4 h in the dark to ensure dispersion of the NPs. The Ag-acetone mixture was then mixed at a 1:1 ratio by weight with pipe cement (PC) (PVC solvent cement, Aquaflow, UK) and vortexed for an additional 30 s. A no particle control solution was prepared by mixing acetone with PC at the same ratio, but with no Ag NPs added. The disks were randomly divided into three groups. The specimens of the first group were left uncoated and assigned as 'uPVC' disks. The disks in the second group were fully coated by carefully pipetting 100 µL of the PC-acetone mixture onto the surface of each face using wide orifice pipette tips; these are referred to as 'PC' disks. The mixture was applied in the form of a very thin layer and was left to air-dry for 10 min between coating each face. The disks in the third group, referred to as 'Ag-PC' disks, were coated with the Ag-acetone and PC mixture using the same technique. The coatings of each Ag-PC disk carried a total mass of 2 mg of Ag (100 µL of a 10 g L<sup>-1</sup> Ag nanosolution applied to each disk face). Both faces of the Ag-PC disks were subsequently ground with a FEPA 800 silicon carbide paper (22 µm grain size, Struers, Denmark) using a Buehler EcoMet 250 grinder-polisher to ensure that Ag NPs were bioavailable and not fully

embedded within the PC matrix. Each face was ground for 30 s and surface finish was assessed visually to ensure consistency across the surface. The PC specimens were also ground so that their surface nanotopography matched that of the Ag-PC disks. All specimens were sterilized by immersion in a 2% NaOCl solution in sterile 50 mL centrifuge tubes on a roller mixer at room temperature for 15 min, followed by triple rinses with sterile deionized water to remove residual hypochlorite.

Further specimens were prepared following the same techniques to be used in the benchtop sink trap model and *in situ* sink trap experiments. For those, an additional hole was created in the center of each disk using a heated nichrome wire (Figure S1). Nichrome wires were then inserted through the disk holes and sections of plastic tubing were used as spacers to ensure exposure of the disk surfaces (Figure S2). The setup allowed disks to remain securely in place when left in the sink traps during the exposure studies.

### 2.2. Disk surface characterization

Surface topography is known to affect early stages of biofilm development (Crawford et al. 2012) and thus the surface roughness of specimens was determined, following the method previously reported by Besinis et al. (2017). The surface roughness of the control and coated disks was quantified by measuring the mean deviation of the roughness profile ( $R_a$ ) and the maximum primary height of roughness profile ( $R_z$ ) using an Olympus LEXT OLS 3000 confocal laser scanning microscope equipped with a 408 nm laser diode class 2 laser. Measurements were conducted using an optical zoom of 1× and a total magnification of 50×. Profiles were Gaussian filtered with a cutoff wavelength value of 85.2 µm. Surface roughness was measured at three different locations on the surface of each disk ( $n=6$  disks/group). Surface nanotopography was further investigated by 3D analysis using the Olympus LEXT OLS 6.0.7 software.

Additional specimens were prepared ( $n=3$  disks/group) for scanning electron microscopy (SEM) analysis to verify the successful application of the coatings and examine the surface morphology of the control and coated disks. Specimens were gold sputtered to increase conductivity and improve image resolution before they were examined with SEM using JOEL JSM-6610 LV equipped with Oxford Instruments Aztec X-Ray analytical system. Low vacuum energy dispersive X-ray spectroscopy (EDS) was also employed to

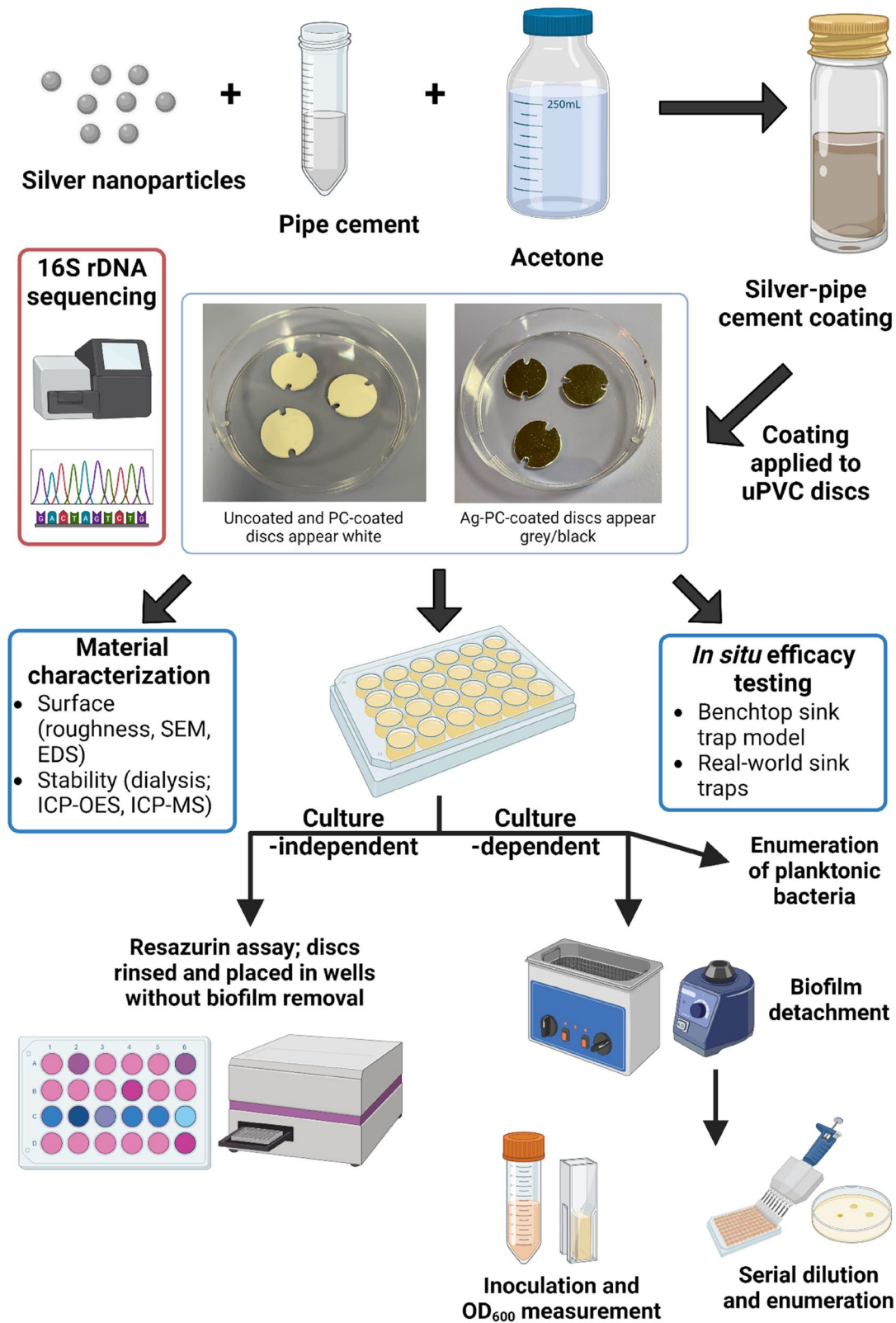


**Figure 1.** Schematic showing a general overview of the workflow from preparation of nanocoatings, material characterization, disk exposure experiments both *in vitro* and *in situ* and assessment of antibacterial activity by culture-dependent and -independent means. Created with BioRender.com.



analyze the elemental composition of the coatings and confirm the presence of Ag NPs. Identical operating conditions and scanning parameter settings were used for all EDS scans (spot size: 10  $\mu\text{m}$ ; accelerating voltage: 10 kV; working distance 10 mm). Data and spectra analysis were achieved using Aztec 2.2 software (Oxford Instruments, Abingdon, UK).

### 2.3. Dissolution of Ag and stability of the antibacterial nanocoatings

The stability of the Ag nanocoatings was initially assessed by measuring the total concentration of dissolved Ag released in ultrapure water by performing a 24 h dialysis study based on the method published previously (Besinis et al., 2014b; Handy, Eddy, and Romain 1989). Additional control and coated disks identical to those used in the exposure experiments were prepared as described above. All glassware, magnetic stirrer bars and dialysis tubing had been acid washed in a 5% nitric acid bath overnight and then triple rinsed in ultrapure Milli-Q water (18.2 M $\Omega$ -cm, Elga, France) prior to the experiment. Dialysis tubing (D9777, cellulose membrane with molecular weight cut off at 12,000 Da, Sigma-Aldrich Ltd, Dorset, UK) with an approximate exclusion size of 2.5 nm was used to make 70 mm long x 25 mm wide dialysis bags which were each filled with 8 mL of Milli-Q water. Disks were individually placed in separate dialysis bags, which were sealed with Medi-clips to prevent any leakage, and then suspended from retort stands such that they were fully immersed in identical glass beakers each containing 492 mL Milli-Q water. Care was taken to select beakers of identical size and shape, and each group was tested in triplicate. The solutions in the beakers were gently agitated with a multipoint magnetic stirrer for 24 h at room temperature. Samples of the external media (4.5 mL) were taken from each beaker at 0, 0.5, 1, 2, 3, 4, 6, 8, and 24 h. Samples were immediately acidified by addition of 100  $\mu\text{L}$  68% (v/v) nitric acid (AnalaR NORMAPUR<sup>®</sup> analytical reagent, VWR, PA, USA), vortexed for 30 s, and stored in sterile plastic containers at 4°C in the dark. At the end of the experiment, the remaining contents of the dialysis bags were also collected, acidified and stored as above. All dialysis samples were analyzed within 24 h to quantify total Ag concentrations using inductively coupled plasma mass spectrometry (ICP-MS) (XSeries, Thermo Scientific, UK) against matrix-matched standards. Sample runs included blanks to correct for instrument drift and procedural blanks to correct for background metal concentrations.

The stability of the Ag-PC nanocoatings was also assessed by measuring the total concentration of Ag in the media at the end of the *in vitro* bacterial exposure studies. Media samples were transferred from the 24-well plates to separate plastic bijoux tubes, mixed 1:1 with 2% (v/v) nitric acid, and stored overnight at 4°C in the dark before being analyzed using inductively coupled plasma optical emission spectroscopy (ICP-OES) (iCAP 7000 series, Thermo Scientific, UK). Suitable blanks and matrix-matched standards were used as above.

### 2.4. Collection and enrichment of hospital sink trap samples

The sink traps ( $n=3$ ) from handwashing sinks located in acute care wards were swabbed using eSwabs with 1 mL liquid amies preservation medium. Specimens were stored immediately at 4°C and transferred to the laboratory within 24 h. Each of the three swabs and the total volume of the preservation medium from each swab were then transferred to separate 5 mL tubes containing 3 mL Dulbecco A phosphate-buffered saline (Thermo Scientific Oxoid, UK) and swabbed material was liberated. All three swab samples were pooled, and the total pooled volume was added to a 250 mL Erlenmeyer flask containing 50 mL Reasoner's 2A broth (prepared in-house identically to Oxoid CM0906, except omitting agar). The flask was incubated at 20°C with shaking at 100 rpm for 3 days under normal atmosphere to enrich bacterial numbers. After three days, the culture was scaled up to 200 mL in a 1000 mL flask in Reasoner's 2A broth and growth continued at 20°C with shaking at 100 rpm for 3 additional days. At the end of enrichment, aliquots of the mixture were prepared for storage having a final concentration of 25% (v/v) glycerol, which were later used for the disk exposure experiments (Section 2.5). The remaining culture was made up to 900 mL by addition of autoclaved tap water from a laboratory cold tap, and the mixture was later used to inoculate the laboratory benchtop sink trap model system (Section 2.6).

### 2.5. Experimental design for *in vitro* disk exposure studies

Single-species cultures of representative bacteria and the mixed-species hospital sink trap cultures were used to assess the antibacterial efficacy of the Ag nanocoating *in vitro*. *Pseudomonas aeruginosa* NCIMB 10817 (ATCC 25619), *Enterococcus faecalis* NCTC 12697

(ATCC 29212), and a clinical isolate of *Acinetobacter baumannii* were cultured on lysogeny broth (LB) media (Fisher Bioreagents™, UK) at 37°C. The strains of *P. aeruginosa* and *E. faecalis* were derived from a collection curated by Mr Matthew Emery at the University of Plymouth, while *A. baumannii* was obtained from University Hospitals Plymouth NHS Trust. These strains were selected as they are among the most common pathogens known to cause nosocomial infections and these bacteria have previously been reported as having been recovered from sink trap samples. Mixed-species cultures consisted of the pooled and enriched mixtures from hospital sink traps (Section 2.4) and a sample of the university building's sink traps (Section 2.7). Generally, the experimental design involved exposing *P. aeruginosa*, *E. faecalis*, *A. baumannii*, or the mixed-species cultures in 24-well microplates for 24 h to the Ag-PC coated disks in comparison to the uncoated uPVC disks (negative control), PC disks (no particle control) and blank controls (no disk in the well). The 24-well microplate was used as the unit of replication ( $n=3$  disks/treatment). Each disk was placed on the bottom of a well acting as the substrate for biofilm formation. Overnight cultures were centrifuged three times at  $4,700\times g$  for 20 min, each time removing the supernatant and resuspending in fresh 1% LB. After the third centrifugation, suspensions were adjusted to an optical density at 600 nm ( $OD_{600}$ ) of 0.1 and used immediately. Each well was inoculated with 150  $\mu$ L of bacterial suspension and 1.35 mL of 1% LB broth to a final volume of 1.5 mL, resulting in a starting bacterial density of  $10^6$  colony-forming units (CFU)  $\text{mL}^{-1}$  in each well. Serial dilutions and Miles and Misra drop counts (Miles, Misra, and Irwin 1938) of inocula were performed on LB agar to confirm initial bacterial density. The microplates were incubated at 37°C for 24 h in the dark on a rotary shaker (120 rpm). At the end of the 24 h exposure, the antiplanktonic and antibiofilm activities of the nanocoatings were assessed by quantifying the viability of bacteria in the media as well as bacteria adhered to the surface of the disks. Briefly, bacterial viability in the media in the microplates was measured by performing serial dilutions and Miles and Misra drop counts on LB agar. The total Ag concentration in the media was measured by ICP-OES to investigate the stability of the nanocoatings applied to the Ag-PC disks (Section 2.3). The disks were then removed from the microplates to assess the extent of biofilm development. That was achieved using the Miles and Misra method as well as running turbidity and resazurin assays (Section 2.8).

## 2.6. Experimental design for evaluating the nanocoatings' antibiofilm efficacy using a laboratory benchtop sink trap model system

New bottle-style sink traps ( $n=3$ ; McAlpine, UK) were cleaned with 70% industrial methylated spirits, and securely set up in an upright position using retort stands on a laboratory bench (Figure S3). The 900 mL of enriched hospital sink trap culture in autoclaved tap water prepared previously (Section 2.4) was used to fill each sink trap with 300 mL, which was the maximum volume they could accommodate. The inlet and outlet ports of the sink traps were sealed with parafilm, and the sink traps were left on the bench for three days at room temperature to allow bacterial attachment and colonization to occur. Following colonization, sink traps were subjected to flushing conditions simulating sink usage by pouring 1 L of autoclaved tap water into each sink trap by the top inlet port and allowing it to flow out from the bottom outlet port. At that stage, disks mounted on nichrome wires (see Section 2.1) were introduced to the sink traps, which marked the baseline for this experiment. Each sink trap contained disks from all experimental groups (uPVC, PC, Ag-PC) mounted on separate nichrome wires so that each sink trap was effectively an experimental replicate. The bacterial densities of sink trap media were routinely monitored every 1–2 days by sampling from the bottom of the trap using a sterile serological pipette inserted through the top inlet port and performing serial dilutions and Miles and Misra drop counts on agar. To maintain a relatively constant bacterial density during the experiment, and to mimic sink usage, sink traps were flushed with 1 L of autoclaved tap water as above when their bacterial densities began to increase. At each endpoint (4, 11 and 25 days), disks ( $n=3$ /treatment) were retrieved aseptically from the wires in the sink traps and the antibiofilm efficacy of the nanocoatings was quantified (Section 2.8).

## 2.7. Experimental design for the in situ testing of the nanocoating antibiofilm efficacy in real-world sink traps

The study was conducted in sink traps located across two university buildings (A and B) between October and December 2021. Building A consisted of staff offices, teaching facilities, a café, and laboratories. Building B consisted of offices but was largely dominated by laboratory space. Four hand-washing sinks were identified across buildings A

and B and their sink traps replaced with identical new bottle-style sink traps (McAlpine, UK) which were assembled and cleaned with 70% industrial methylated spirits upon receipt. Sink trap 1 (ST1) and ST2 were in building A, located in two male toilets on different floors (ST2 was directly above ST1) with a layout including 3 urinals and 2 cubicles (see [Figure S4](#)). ST3 and ST4 were in building B, in neighboring male and female toilets respectively, with a single toilet each (see [Figure S5](#)). ST1–4 were all fitted to handwashing sinks during periods of active building use. Disks were mounted on nichrome wires and placed in ST1–4 following the same experimental design as in the study using the laboratory benchtop sink trap model system (above). At baseline, and after the collection of disks at each endpoint (1, 2, 7, 14, 28 days), the tap was left to run for 30 s to refill the traps with water. Disks were analyzed by detachment and enumeration of biofilm-derived cells and resazurin assay as described below. After the final endpoint, 10 mL samples and swabs were collected from ST1–4 and pooled for *in vitro* disk exposure experiments ([Section 2.5](#)), and for DNA extractions and 16S rRNA gene sequencing ([Section 2.9](#)).

## 2.8. Assessment of antibiofilm efficacy

The viability of the bacteria adhered to the control and coated uPVC disks was assessed by following the protocol described by Besinis et al. (2017). In brief, disks were removed from the 24-well plates or sink traps at the end of the *in vitro* or *in situ* exposure studies, respectively. Each face of the disks was aseptically rinsed with 3 mL of sterile saline (0.85% NaCl) to remove non-adherent bacteria. Each disk was then transferred to a separate glass vial containing 2 mL sterile saline. Vials were vortexed for 5 s, sonicated by immersion in an ultrasonic bath (35 kHz, Fisherbrand FB 11010, Germany) for 60 s and then vortexed for an additional 5 s. Afterwards, 0.5 mL of the media from the sonicated disks from each vial was added to 4.5 mL LB broth and incubated for 5 h at 37°C with 120 rpm agitation. At the end of the 5 h incubation, turbidimetric values were measured to quantify the regrowth of biofilm-derived bacteria using a spectrophotometer (BioPhotometer, Eppendorf, Germany) at 600 nm. Aliquots of the contents of each vial containing detached biofilm were serially diluted and bacterial density enumerated by Miles and Misra drop counts on LB agar to determine antibiofilm efficacy. The resazurin assay was also employed for the *in situ* assessment of the

biofilm development on the surface of the disks without the need of using sonication to remove attached bacteria. The method followed was as previously described (Travnickova et al. 2019); resazurin stock solutions were prepared at 20 mM using sterile 0.85% NaCl and stored at –20°C until use, when they were thawed and diluted in 0.85% NaCl to 20 µM. Control and coated disks were rinsed as described above to remove non-adherent bacteria and then each immersed in 2 mL of 20 µM resazurin solution in a 24-well plate and incubated statically in the dark at 37°C. After 4 h, 200 µL aliquots in triplicate were transferred to 96-well microtitre plates, which were analyzed by a FLUOstar Omega microplate reader (BMG Labtech, UK) applying an excitation wavelength of 544 nm, emission wavelength of 590 nm, and gain set at 700. A pilot study was initially conducted to confirm that *in situ* biofilm could be quantified by resazurin ([Figure S6](#)) and that the production of fluorescence was proportional to the bacterial load ([Figure S7](#)). Tenfold serial dilutions of an *A. baumannii* culture were prepared in 20 µM resazurin solution and 200 µL per well transferred to a 96-well microtitre plate in sextuplicate per dilution. The plate was incubated in the FLUOstar Omega microplate reader at 37°C and assessed by a kinetic measurement every 30 min for 13 h using the settings described above.

## 2.9. 16S rRNA gene amplicon sequencing

Sequencing of 16S rRNA gene amplicons following PCR of extracted DNA was performed to characterize the bacterial community present in sink traps. Aliquots were taken after the pooling and enrichment steps following receipt of the hospital sink trap swabs and these were archived at –80°C. Samples of the contents of ST1–4 were also taken, pooled, and archived at –80°C. Metagenomic DNA was extracted from 250 µL of each sample using the DNeasy® PowerSoil® Pro kit (Qiagen, Germany) according to the manufacturer's instructions. Extraction yield was quantified using the Qubit™ dsDNA HS assay kit (Invitrogen, MA, USA) and purity was determined using a Nanodrop™ spectrophotometer (Thermo Fisher Scientific, UK). DNA samples that met the quality criteria were provided to Novogene (China) for PCR amplification, product quantification, purification, library preparation and Illumina sequencing. The target hypervariable regions were V3–4 using primers 341 F and 806 R (Takahashi et al. 2014; Muyzer, de Waal, and Uitterlinden 1993; Caporaso et al. 2011; Hiergeist, Reischl, and Gessner 2016)



(341 F: CCTAYGGGRBGCASCAG and 806 R: GGACTACNNGGGTATCTAAT) and V4–5 using primers 515F and 907R (Caporaso et al. 2011; Edwardson and Hollibaugh 2018; Armitage et al. 2012; Chen et al. 2017; Hugerth et al. 2020), (515 F: GTGCCAGCMGCCGCGGTAA and 907 R: CCGTCAATTCCTTTGAGTTT). Degenerate bases were universal, as follows: Y=C/T, B=C/G/T, S=C/G, N=A/C/G/T, M=A/C. Novogene used a proprietary bioinformatic pipeline to merge and filter data and conduct operational taxonomic unit clustering.

## 2.10. Statistics

All data are presented as mean  $\pm$  standard deviation values. Statistical analysis was performed using GraphPad Prism version 8.4.3 for Mac (GraphPad Software, Inc., USA). The Shapiro-Wilk normality test was used prior to applying parametric testing. Differences between control and test groups were evaluated using one-way analysis of variance (one-way ANOVA, Tukey's *post hoc* test). Differences among the control and coated specimens (treatment effect) over time, at different temperatures or against different pathogens were evaluated using two-way analysis of variance (two-way ANOVA, Tukey's *post hoc* test). All statistical analysis used a 95% confidence limit, so that  $p$  values  $\geq 0.05$  were not considered statistically significant.

## 3. Results

### 3.1. Surface characterization

Prior to assessing the antibacterial properties of the nanocoatings applied to the uPVC disks, surface roughness measurements of the control and different test groups were taken using confocal microscopy (Table 1) as surface topography is known to affect early stages of biofilm development (Crawford et al. 2012). Application of the PC coating did not result

**Table 1.** Surface roughness values of the uncoated control and coated disks.

Type of nanocoating	$R_a$ ( $\mu\text{m}$ )	$R_z$ ( $\mu\text{m}$ )
Uncoated uPVC control	$0.327 \pm 0.052^a$	$2.352 \pm 0.645^a$
PC control (unground)	$0.474 \pm 0.237^{ab}$	$3.004 \pm 0.984^a$
PC control (ground)	$2.009 \pm 0.344^c$	$12.684 \pm 2.328^b$
Ag-PC (unground)	$0.659 \pm 0.101^b$	$4.514 \pm 1.238^c$
Ag-PC (ground)	$1.552 \pm 0.369^d$	$10.867 \pm 2.172^d$

Measurements from three different sites on the surface of each disk ( $n=6$  disks/treatment) were taken (total magnification  $50\times$ ). uPVC, unplasticized polyvinyl chloride; PC, pipe cement coating; Ag-PC, Silver-pipe cement coating. Data are expressed as mean  $\pm$  S.D. Different letters indicate significant differences between the test groups within each metric (one-way ANOVA with Tukey's *post hoc* test,  $p < 0.05$ ).

in significantly higher surface roughness values compared to the uncoated controls ( $p > 0.05$ ). Addition of Ag NPs to the PC coatings (Ag-PC) did not cause an increase in  $R_a$  values ( $p > 0.05$ ) but both  $R_a$  and  $R_z$  values were significantly higher compared to the uncoated controls ( $p < 0.05$ ). The highest surface roughness values were recorded for the ground surfaces with differences being significant compared to unground coatings and uncoated controls ( $p < 0.05$ ). The three-dimensional images of the surface morphology confirmed these findings (Figure 2). The surface of the uncoated uPVC disks appeared to be visually flat and smooth (Figure 2A). Images indicated that application of the coatings produced rougher surfaces, but the surfaces of the PC and Ag-PC disks appeared very similar (Figure 2B,C). However, the grinding process introduced scratches and grooves, which was expressed by an evident increase in surface roughness (Figure 2D).

SEM images were also obtained to verify the surface topography of the specimens (Figure 3). The SEM analysis confirmed the successful application of the coatings showing the surface of all specimens fully and evenly covered, without any discontinuities. The surfaces of the uPVC, PC and Ag-PC specimens were relatively featureless, but grooves and scratches were introduced as a result of the grinding process used in order to expose the Ag NPs embedded within the pipe cement matrix (Figure 3A–E). The backscattered SEM images revealed the distribution of Ag NPs in the coatings. Agglomerates of Ag NPs were visible within the PC matrix but also on the surface of the Ag-PC specimens following surface grinding (Figure 3I,J). Those Ag NPs clusters appeared as bright areas in the images because of the higher atomic number of Ag compared to the other chemical elements present in the coatings. The EDS spectra obtained confirmed the elemental composition of the coatings and the presence of Ag NPs in the Ag-PC nanocoatings (Figure 3F–J). Quantitative analysis showed that the weight percentages of Cl, Si, Ti and Ag were 30, 5, 2 and 3% respectively, when the frame scan mode was selected. The weight percentage of Ag increased to 30% when the spot scan mode was selected targeting the bright areas shown in Figure 3I,J.

### 3.2. Nanocoating stability and dissolution of silver in ultrapure water

A 24 h dialysis study was conducted to assess the stability of the Ag nanocoatings by measuring the release of Ag when specimens were immersed in

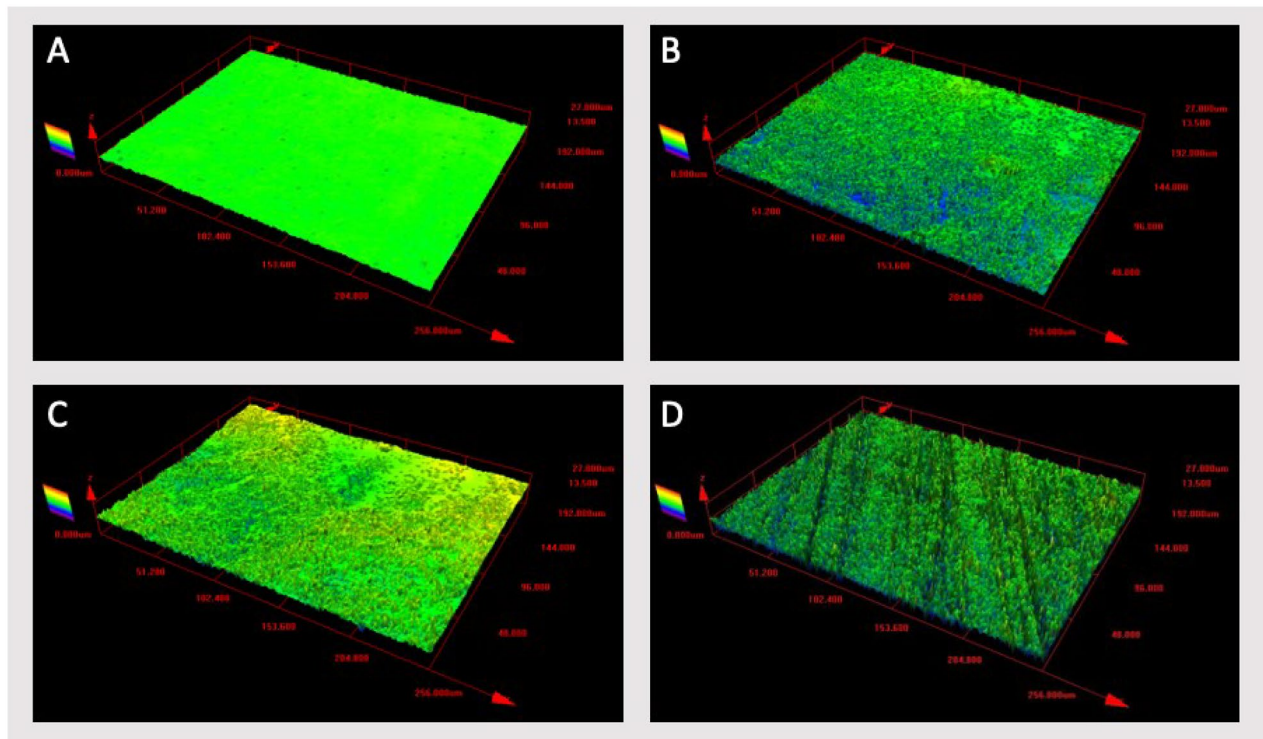


**Figure 2.** Representative three-dimensional images showing the surface topography of uncoated unplasticized polyvinyl chloride (uPVC) disks (a), uPVC disks coated with pipe cement alone as a no particle control (B), uPVC disks coated with pipe cement and silver nanoparticles (Ag NPs) without a grinding step (C), and uPVC disks coated with pipe cement and Ag NPs followed by a grinding step with FEPA 800 silicon carbide paper (D). Images acquired by an olympus LEXT OLS 3000 confocal laser scanning microscope equipped with a 408nm laser diode class 2 laser (total magnification: 50 $\times$ ). In each image, the limit of the x-axis is 256  $\mu$ m, the y-axis is 192  $\mu$ m, and the z-axis is 27  $\mu$ m.

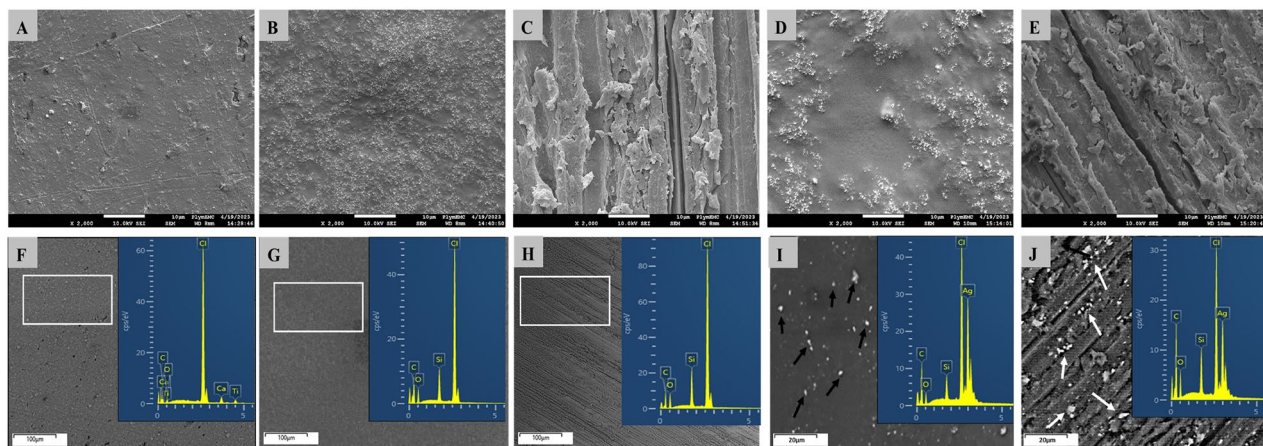


**Figure 3.** Representative scanning electron micrographs ( $\times 2.0k$  magnification) showing the surface topography of (A) uncoated unplasticized polyvinyl chloride (uPVC) disks, (B) uPVC disks coated with pipe cement, (C) uPVC disks coated with pipe cement following surface grinding, (D) uPVC disks coated with pipe cement containing silver nanoparticles (Ag NPs), (E) uPVC disks coated with pipe cement containing Ag NPs following surface grinding. Backscattered images (F–J) demonstrate elements with different atomic numbers present in the coatings and align vertically with scanning electron micrographs. Black arrows indicate the locations of Ag NPs within the pipe cement matrix appearing as brighter areas (I). White arrows indicate the locations of Ag NPs within and on the surface of the Ag-PC coating following surface grinding (J). The spectra shown in the insets in panels F–J were obtained by energy dispersive x-ray spectroscopy (EDS) and show the elemental composition of the uncoated uPVC (F), unground pipe cement coating (G), ground pipe cement coating (H), unground pipe cement with Ag NPs coating (I) and ground pipe cement with Ag NPs coating (J).

ultrapure (Milli-Q) water. ICP-MS measurements showed that the total release of Ag from the Ag-PC nanocoatings at the end of the 24 h study was very low and not discernible from the uPVC and PC groups, which were employed as no particle controls. Therefore, Ag dissolution was negligible, suggesting very high stability of the Ag-PC nanocoatings (Figure 4).

The final (24 h) Ag concentration measurements for the Ag-PC (unground) and Ag-PC (ground) groups were  $0.115 \pm 0.036$  and  $0.098 \pm 0.037 \mu\text{g L}^{-1}$ , respectively. The theoretical maximum Ag concentration that could have been recorded, if the total amount of Ag present in the Ag-PC nanocoatings (2 mg) applied to both sides of each uPVC disk was fully dissolved or dislodged, would equate to  $4 \text{ mg L}^{-1}$  ( $4,000 \mu\text{g L}^{-1}$ ). Therefore, the total release of dissolved Ag in Milli-Q water after 24 h were just 0.003% and 0.002% for the Ag-PC (unground) and Ag-PC (ground) coatings, respectively. Higher Ag concentrations were measured when the contents of the dialysis bags (8 mL volumes) were analyzed at the end of the dialysis experiment;  $1.360 \pm 0.876$  and  $1.838 \pm 1.348 \mu\text{g L}^{-1}$  for Ag-PC (unground) and Ag-PC (ground) nanocoatings,

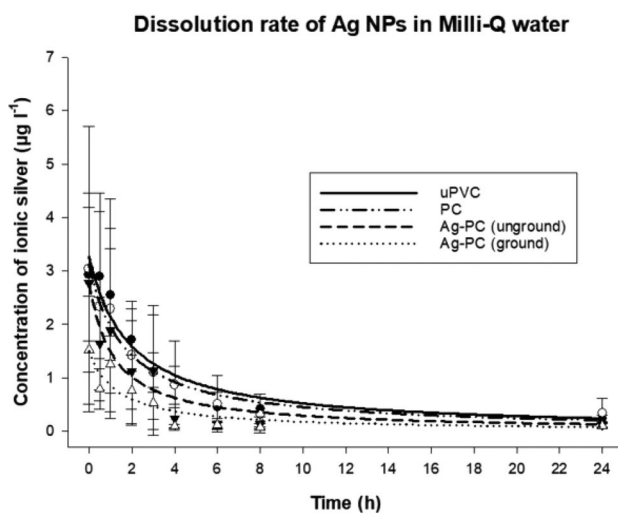


**Figure 4.** Dialysis curves showing the total release of dissolved silver (Ag) from the control and coated uPVC disks over a 24 h period in Milli-Q ultrapure water. Concentrations were determined by inductively coupled plasma mass spectrometry (ICP-MS) expressing stability of the coatings. uPVC, unplasticized polyvinyl chloride; PC, pipe cement coating; Ag-PC, silver-pipe cement coating. Data are means  $\pm$  S.D.,  $n=3$  replicates per group. Curves were fitted using SigmaPlot 14.5 (systat Software, Inc.) applying the hyperbolic decay two parameter equation on the raw data. (uPVC)  $y = (3.27 \cdot 1.90)/(1.90 + x)$ , (PC)  $(3.12 \cdot 1.68)/(1.68 + x)$ , (Ag-PC unground)  $(2.76 \cdot 1.17)/(1.17 + x)$ , (Ag-PC ground)  $(1.50 \cdot 1.32)/(1.32 + x)$ . All four curves are practically superimposed since silver ion release was very low.

respectively. These increased values reflected the amount of Ag that remained trapped inside the dialysis bags, presumably in particulate form. However, the sum of the amount of Ag released inside the dialysis bags as well as the external compartment of the beakers was  $0.063 \mu\text{g}$ , which means that the percentage of Ag release in the total volume of ultrapure water in the beaker remain virtually unchanged, at 0.003% for both Ag-PC (ground) and Ag-PC (unground) groups. In practice, Ag leaching from the nanocoatings was negligible with no significant differences when compared to the uPVC or PC controls.

### 3.3. Silver nanocoating stability in bacterial culture media

During the *in vitro* bacterial exposures, specimens were immersed in 1% LB media and therefore exposed to a variety of ions, proteins and bacterial metabolites that could affect the stability of nanocoatings differently compared to ultrapure water. Samples were collected from the media in the microplates at the end of the exposure studies and analyzed with ICP-OES to quantify the Ag release from the Ag-PC nanocoatings into the surrounding media (Table 2).

The Ag release from the Ag-PC nanocoatings was relatively consistent across experiments with different bacterial species. The total concentrations of Ag leaching from the Ag-PC nanocoatings after 24 h were  $1.308$ ,  $0.999$  and  $1.365 \text{ mg L}^{-1}$  for the coated disks exposed to *P. aeruginosa*, *A. baumannii* and *E. faecalis*, respectively (Table 2). The levels of Ag detection for the groups not containing Ag (Media only, uPVC, PC) were very low, around the detection limit of the ICP-OES instrument ( $0.009 \text{ mg L}^{-1}$ ). In the 24-well microplate setup (media volume of  $1.5 \text{ mL/well}$ ), the theoretical maximum concentration of Ag in each well following complete dissolution of the Ag present in the Ag-PC nanocoatings ( $2 \text{ mg}$ ) would equate to  $1,333 \text{ mg L}^{-1}$ . Using this value as a reference, the total release of dissolved Ag when Ag-PC specimens were exposed to the media was 0.098%, 0.075% and 0.102% of the total Ag present on disks for *P. aeruginosa*, *A. baumannii* and *E. faecalis*, respectively.

Analysis of the media following sonication of the nanocoated disks to remove bacteria adhered to the surfaces as part of the enumeration of biofilm-derived cells also demonstrated low Ag concentrations ( $0.308 \pm 0.044$ ,  $0.376 \pm 0.040$  and  $0.344 \pm 0.028 \text{ mg L}^{-1}$  for Ag-PC specimens exposed



**Table 2.** Silver release following exposure of disks to bacterial inocula.

Type of coating	Concentration of silver in 1% LB media after 24h (mg L <sup>-1</sup> )		
	<i>Pseudomonas aeruginosa</i>	<i>Acinetobacter baumannii</i>	<i>Enterococcus faecalis</i>
Media only	0.011 ± 0.002 <sup>a</sup>	0.007 ± 0.005 <sup>a</sup>	0.014 ± 0.002 <sup>a</sup>
uPVC	0.012 ± 0.002 <sup>a</sup>	0.009 ± 0.005 <sup>a</sup>	0.016 ± 0.004 <sup>a</sup>
PC	0.012 ± 0.001 <sup>a</sup>	0.009 ± 0.005 <sup>a</sup>	0.014 ± 0.001 <sup>a</sup>
Ag-PC	1.308 ± 0.069 <sup>b</sup>	0.999 ± 0.372 <sup>b</sup>	1.365 ± 0.089 <sup>b</sup>

Concentration of silver in 1% lysogeny broth (LB) media as measured by inductively coupled plasma optical emission spectrometry (ICP-OES) following 24h exposure to bacterial inocula at 37 °C. uPVC, unplasticized polyvinyl chloride; PC, pipe cement coating; Ag-PC, Silver-pipe cement coating. Data are expressed as means ± S.D., *n* = 3 biological replicates. Different letters indicate significant differences at *p* < 0.05 for all comparisons (two-way ANOVA followed by Tukey's *post hoc* test).

to *P. aeruginosa*, *A. baumannii* and *E. faecalis*, respectively), which further confirmed nanocoating stability. Ag release as a result of the sonication process remained less than 0.04% of the total Ag present in the coatings. This step was performed to ensure that the sonication process was not liberating significant additional Ag that could then affect the enumeration of biofilm-derived cells, as well as to give an additional indication of stability.

### 3.4. Potent antibiofilm and antiplanktonic activity *in vitro* against *P. aeruginosa*, *A. baumannii*, *E. faecalis* and hospital sink trap bacteria

The extent of *in vitro* antibiofilm and antiplanktonic activity against three representative single-species inocula, and a multispecies hospital sink trap bacterial community (see section about characterization of this community below), was quantified by enumeration following biofilm detachment (Figure 5A–D), by regrowth comparison of detached biofilm cells in broth (Figure 5E–H), biofilm development measured *in situ* using the resazurin assay (Figure 5I–L), and planktonic bacteria enumerated from the media (Figure 5M–P).

The log<sub>10</sub> reductions in culturable biofilm-derived cells between the uPVC and Ag-PC groups were 3.9 for *P. aeruginosa* (Figure 5A), 7.2 for *A. baumannii* (Figure 5B), 2.9 for *E. faecalis* (Figure 5C), and 7.3 for hospital sink trap bacteria (Figure 5D). In all cases, the number of bacteria attached to the Ag-PC nanocoatings were significantly less compared to the uPVC controls (*p* < 0.0001). As an additional assessment of the extent of biofilm formation on the surface of the disks, detached biofilm cells were reinoculated in broth and incubated for 5h followed by quantification of OD<sub>600</sub> (Figure 5E–H). Significantly reduced regrowth was observed for the Ag-PC

nanocoatings for all three bacterial species and the hospital bacterial community (*p* < 0.0001).

The extent of biofilm formation on disks was further determined by application of the resazurin assay, wherein actively metabolizing cells reduce resazurin to the fluorescent product resorufin. This assay was conducted by directly immersing the disks in a resazurin solution, without prior biofilm removal, and incubating for 4h before measurement of fluorescence in order to quantify *in situ* biofilm. The results of the pilot experiments showing the production of resorufin from *in situ* *A. baumannii* biofilms and a kinetic measurement of fluorescence from varying starting bacterial inocula can be found in Figures S6 and S7, respectively. While fluorescent measurements (relative fluorescence units, RFU) obtained from the uncoated control uPVC surfaces for *P. aeruginosa* (Figure 5I), *E. faecalis* (Figure 5J) and hospital sink trap bacteria (Figure 5L) were relatively similar to each other (1743, 2605 and 2343 RFU, respectively), *A. baumannii* (Figure 5J) gave far higher readings (9389 RFU). Resazurin assay results showed there was significantly increased biofilm development on the surfaces of uPVC and PC specimens for all three bacterial species and the hospital bacterial community tested compared to the Ag-PC coated disks (*p* < 0.0001). The level of detected fluorescence from the Ag-PC coated disks was not significantly elevated (*p* > 0.05) above the assay control (resazurin only, to account for background fluorescence and reduction to resorufin in the absence of bacteria), indicating that no biofilm formation was detected on Ag-PC coated disks.

In addition to examining the antibiofilm efficacy of the Ag nanocoatings, their antiplanktonic activity was also investigated with the Ag-PC nanocoatings exhibiting significantly lower CFU counts compared to the other groups. The log<sub>10</sub> reductions in culturable planktonic cells between the uPVC and Ag-PC groups were 2.4, 4.5, 2.9 and 4.4 for *P. aeruginosa* (*p* < 0.0001), *A. baumannii* (*p* < 0.0001), *E. faecalis* (*p* < 0.01) and hospital sink trap bacteria (*p* < 0.0001), respectively (Figure 5M–P). Therefore, Ag-PC nanocoatings were found to have not only strong antibiofilm activity, but also significantly reduce bacterial viability in proximity to the coated surfaces.

### 3.5. Characterization of hospital sink trap swabs by 16S rRNA gene amplicon sequencing

In preparation for experiments using real-world samples, the microbial community in hospital sink traps was examined using 16S rRNA gene amplicon



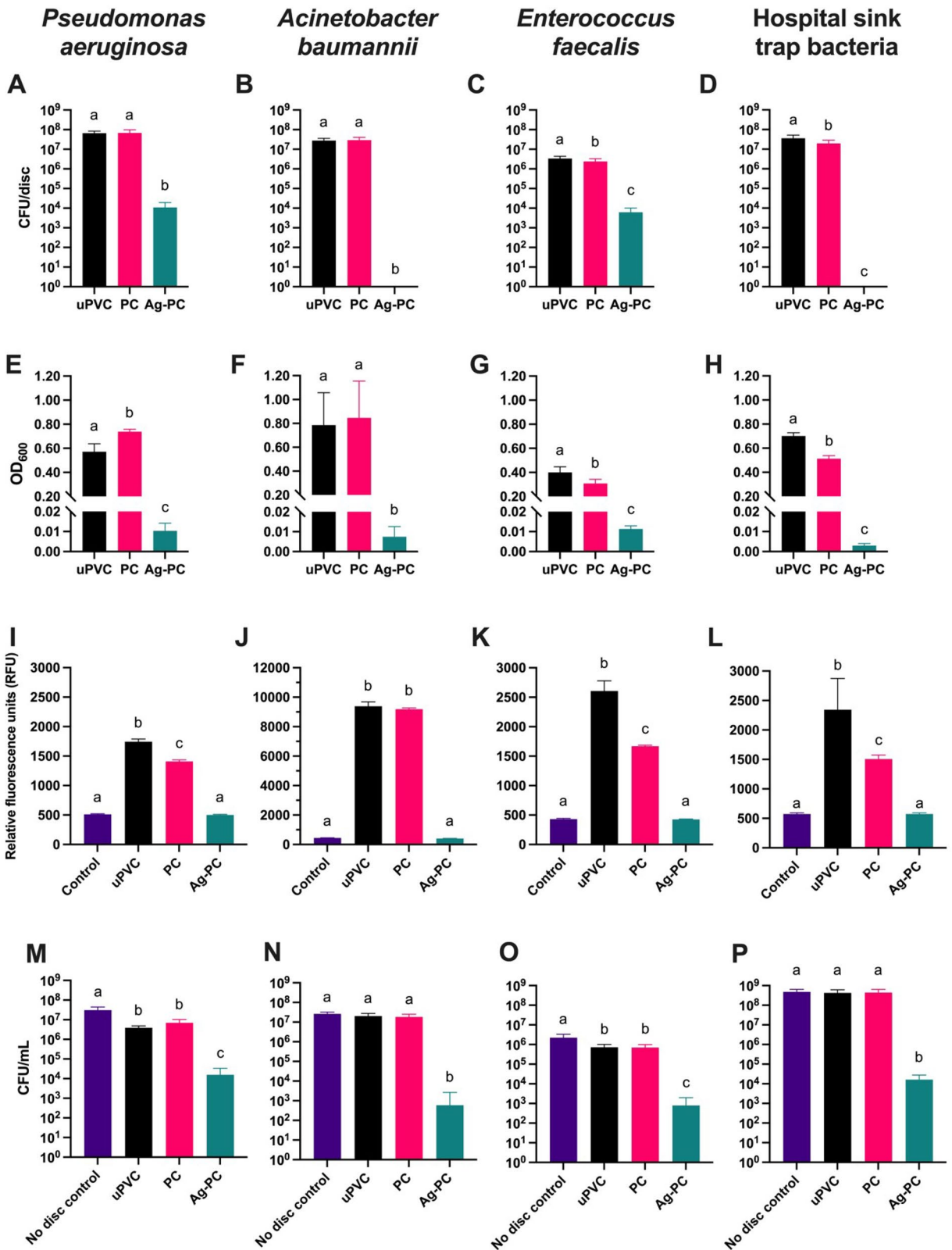


**Figure 5.** Antibacterial efficacy of silver nanocoated disks in an *in vitro* plate-based model against three representative bacterial species (*P. aeruginosa*, *A. baumannii*, *E. faecalis*) and an enriched hospital sink trap bacterial community. Extent of biofilm formation after 24h was measured by enumeration of detached biofilm cells (A–D), by re-inoculating detached biofilm bacteria in broth and measuring optical density at 600 nm (OD<sub>600</sub>) after 5h incubation (E–H), and by the resazurin assay to detect biofilm on disks *in situ* (I–L). Antiplanktonic effect was measured by enumeration of planktonic bacteria (M–P). CFU, colony-forming units; uPVC, unplasticized polyvinyl chloride; PC, pipe cement coating; Ag-PC, silver-pipe cement coating. Data presented as means  $\pm$  S.D.,  $n=3$  biological replicates. Different letters indicate significant differences between the test groups (one-way ANOVA with tukey's *post hoc* test,  $p < 0.05$ ).

sequencing for identification of the taxa present. The genus-level identities, determined by sequencing of two different hypervariable regions (V3–4 and V4–5) of pooled samples without and with enrichment can be found in Figure 6 (full 16S rRNA gene amplicon sequencing results for the pooled group can be found in Table S1). The total number of reads for the V3–4 region were 125,980 and 130,724, and for the V4–5 region were 104,371 and 112,785, for ‘pooled’ and ‘pooled and enriched’, respectively.

The pooled hospital sink trap community was clearly dominated by *Citrobacter* (31.3% and 28.9%), *Pseudomonas* (19.8% and 33.0%), *Serratia* (15.6% and 17.5%), and *Azospira* (6.6% and 6.9%). Enrichment led to significant increases in the proportion of *Serratia* and *Delftia* and corresponding reductions in *Citrobacter* and *Pseudomonas*. Sequencing of the V3–4 region also indicated expansion of the proportions of *Enterobacter*, *Vicinamibacteraceae* and *Elizabethkingia* (Figure 6 and Table S1).

### 3.6. Antibiofilm efficacy against a hospital sink trap biofilm community using a benchtop sink trap model

The longer term antibiofilm efficacy of the nano-coatings was investigated by quantifying biofilm

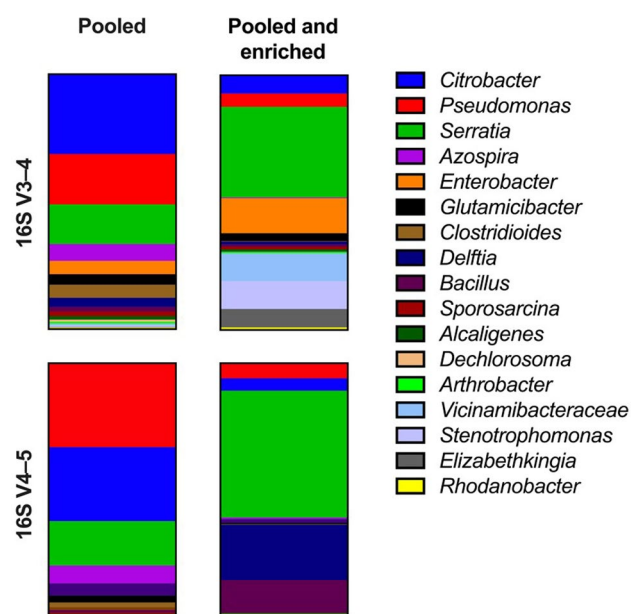


**Figure 6.** Classification of the taxa present in pooled hospital sink trap swab samples alone and following enrichment in reasoner’s 2A broth, as determined by sequencing of two different 16S rRNA gene hypervariable regions (V3–4 and V4–5).

formation on disks incubated for up to 25 days in benchtop sink traps inoculated with the hospital sink trap bacterial community (Figure 7).

Resazurin assay results and CFU counts (Figure 7) confirmed that biofilm development on the Ag-PC disks remained significantly lower compared to the uncoated uPVC disks Ag-PC disks after 4 and 11 days ( $p < 0.01$ ). However, measurements taken after 25 days showed that the antibiofilm effect of the Ag-PC nano-coatings diminished over time with differences not being significant between groups at the final endpoint ( $p > 0.05$ ). The gradual weakening of the antibiofilm activity exhibited by the Ag-PC nano-coatings was corroborated by CFU counts of biofilm-derived bacteria taken on day 25.

The density of planktonic bacteria within the benchtop sink traps was routinely monitored by enumeration during this study. The mean density at baseline was  $2.0 \times 10^8$  CFU mL<sup>-1</sup>, and the mean

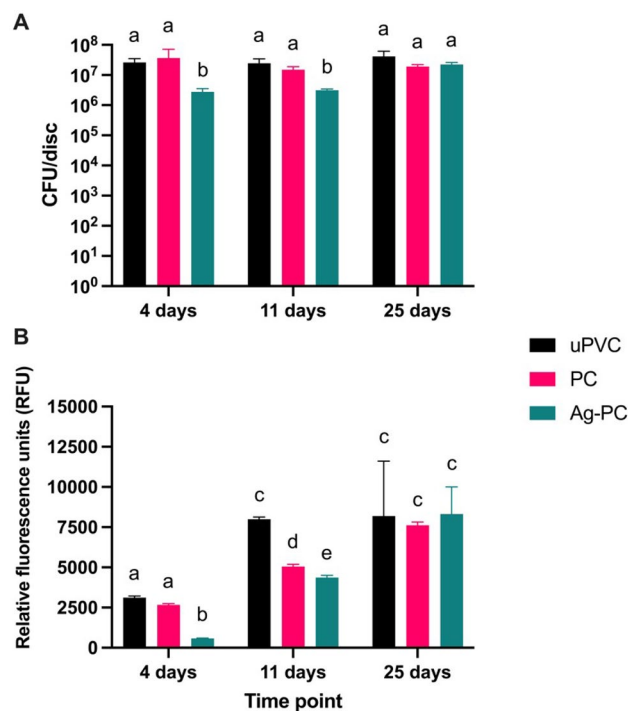


**Figure 7.** Antibiofilm efficacy of silver nano-coated disks in a benchtop sink trap model inoculated with a hospital sink trap bacterial community. Biofilm formation was quantified by colony counts of detached biofilms from disks (A) and by resazurin assay *in situ* on disks without requiring biofilm removal (B). CFU, colony-forming units; uPVC, unplasticized polyvinyl chloride; PC, pipe cement coating; Ag-PC, silver-pipe cement coating. Data presented as means  $\pm$  S.D., from  $n = 3$  independent sink traps. Different letters indicate significant differences at  $p < 0.05$  for all comparisons between the test groups across endpoints (two-way ANOVA followed by Tukey’s *post hoc* test).

densities were  $6.5 \times 10^7$ ,  $1.1 \times 10^8$  and  $2.6 \times 10^7$  CFU mL<sup>-1</sup> on days 4, 11 and 25, respectively.

### 3.7. Characterization of the university building sink trap bacterial community

To further evaluate the utility of the Ag-PC coated surfaces for prevention of biofilm formation, sites were selected that would allow deployment of disks in sink traps in routine use. In preparation for this, samples were recovered from four university building sink traps (ST1–4). These were pooled and subjected to 16S rRNA gene amplicon sequencing for identification of the taxa present (Figure 8). The total number of reads shown in the graphs in Figure 8 were 70,364 for V3–4 and 120,657 for V4–5.

The university building sink traps were largely dominated by *Citrobacter* (65.6% and 87.7% for V3–4 and V4–5 regions, respectively), with V3–4 sequencing indicating other genera such as *Desulfovibrio* (11.7%), *Dethiosulfovibrio* (7.6%) and *Anaerophaga* (3.5%) also being present while V4–5

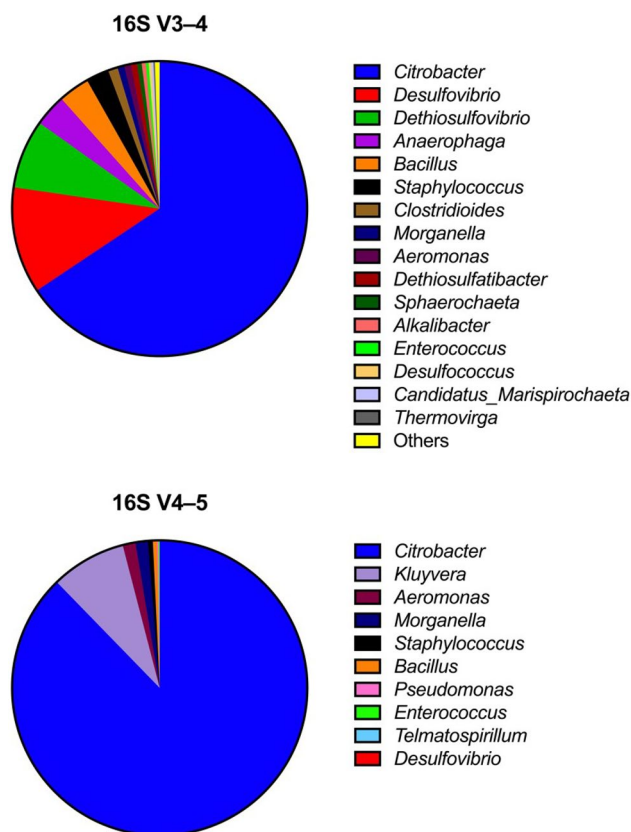


**Figure 8.** Classification of the taxa present in pooled samples from university building sink traps used for *in situ* testing of nanocoatings in real-world sink traps. Classification was achieved by conducting 16S rRNA gene amplicon sequencing of V3–4 and V4–5 hypervariable regions.

sequencing indicated that *Kluyvera* (8.2%) was also present (Figure 8). Overall, when considering genera with >50 reads, diversity compared to the hospital sink trap samples was reduced with 4.8-fold fewer total genera represented ( $n=86$  for hospital sink traps versus  $n=18$  for university building sink traps).

### 3.8. Antibiofilm and antiplanktonic activity of nanocoatings against the university building sink trap bacterial community tested in vitro

The efficacy of the Ag-PC nanocoatings against the specific bacterial community from sink traps in the university building was determined by running additional 24 h exposure studies. These experiments were conducted at both room temperature and 37°C to investigate whether an elevated temperature would affect the antibacterial action of the nanocoatings (Figure 9). Microplates hosting disks from the control and test groups were inoculated with contents from the sink traps and measurements were taken 24 h later using the resazurin assay and CFU enumeration. Regardless of the test temperature, results showed that Ag nanocoatings had evident antibiofilm and antiplanktonic activity which was expressed by significantly reduced biofilm development on the Ag-PC disks ( $p < 0.0001$ ) and significantly reduced bacterial viability in the surrounding media ( $p < 0.001$ ) when compared to the uncoated (uPVC) and no particle (PC) controls. The mean log<sub>10</sub> reductions in biofilm formation conferred by the Ag nanocoatings were 3.6 (room temperature) and 2.4 (37°C) (Figure 9A). *In situ* investigation of biofilm development using the resazurin assay showed that complete biofilm inhibition was achieved on the surface of the Ag-PC disks for both temperatures tested (Figure 9B). The mean log<sub>10</sub> reductions in culturable planktonic bacteria were 4.3 (room temperature) and 1.8 (37°C) (Figure 9C) suggesting that the antimicrobial action of the Ag-PC specimens was not limited to the very surface of the nanocoatings, presumably due to the small amount of Ag release that was detected.

### 3.9. Antibiofilm activity of nanocoatings in real-world sink traps tested in situ

Additional disks were placed in real-world sink traps ( $n=4$ , ST1–4) across two university buildings to investigate the antibiofilm efficacy of the Ag nanocoating under realistic usage and conditions (Figure 10).

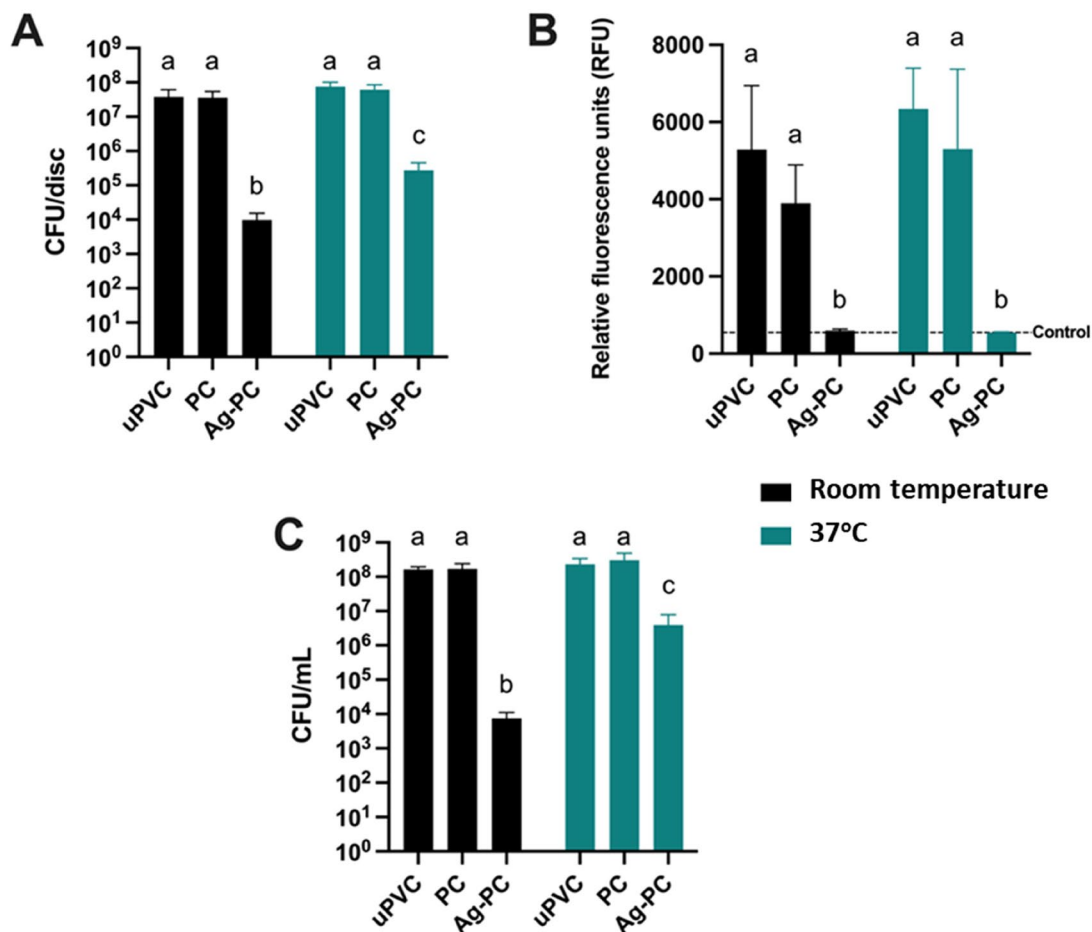


**Figure 9.** Antibacterial efficacy of silver nanocoated disks in an *in vitro* plate-based model where wells were inoculated with the bacterial community from the buildings' sink traps (ST1–4) and disks were exposed for 24 h at room temperature and 37°C. Extent of biofilm formation was measured by enumeration of detached biofilm bacteria (a), by the resazurin assay to detect biofilm on disks *in situ* (B), and by enumeration of planktonic bacteria (C). 'Control' line in (B) indicates fluorescence in wells containing resazurin solution alone, to account for background fluorescence and background reduction of resazurin in these conditions. CFU, colony-forming units; uPVC, unplasticized polyvinyl chloride; PC, pipe cement coating; Ag-PC, silver-pipe cement coating. Data presented as means  $\pm$  S.D.,  $n=3$  biological replicates. Different letters indicate significant differences at  $p < 0.05$  for all comparisons between the test groups at room temperature and 37°C (two-way ANOVA followed by Tukey's *post hoc* test).

The extent of biofilm development on different control and test groups was quantified by classical enumeration of CFUs following detachment of bacterial biofilms (Figure 10A–D), as well as by application of the resazurin assay to quantify biofilm formation on the surface of the disks *in situ* (Figure 10E–H). Results of both assays for ST1 and ST2 in building A showed no biofilm inhibition on the surface of the Ag-PC coated disks for the first 48 h. Results of the remaining endpoints were not as consistent across all the sink traps tested. However, resazurin measurements for ST1 taken on days 7 and 14 clearly demonstrated significantly reduced biofilm formation on Ag-PC coated disks compared to uPVC and PC groups ( $p < 0.0001$ ). Any antibiofilm effect observed earlier for the Ag-PC nanocoatings was not confirmed at the final endpoint (day 28) of this *in*

*situ* study by CFU counts ( $p > 0.05$ ), although resazurin assay data from ST1 indicated that the antibiofilm activity of the Ag-PC nanocoatings remained strong even after 28 days ( $p < 0.01$ ). Resazurin assay data for ST2 also showed reduced biofilm development on the surface of the Ag-PC disks on days 7, 14 and 28, but any differences were statistically significant only for day 7 ( $p < 0.0001$ ). For those Ag-PC disks exposed to the conditions in ST3 located in building B (Figure 10C,G), no antibiofilm effect was observed compared to the control groups ( $p > 0.05$ ). *In situ* assessment of biofilm development by the resazurin assay showed that Ag-PC disks in ST4 exhibited reduced bacterial attachment on their surface when compared to uPVC and PC groups on days 7 and 14 (Figure 10H), but with differences being statistically significant only for day 7 ( $p < 0.0001$ ).



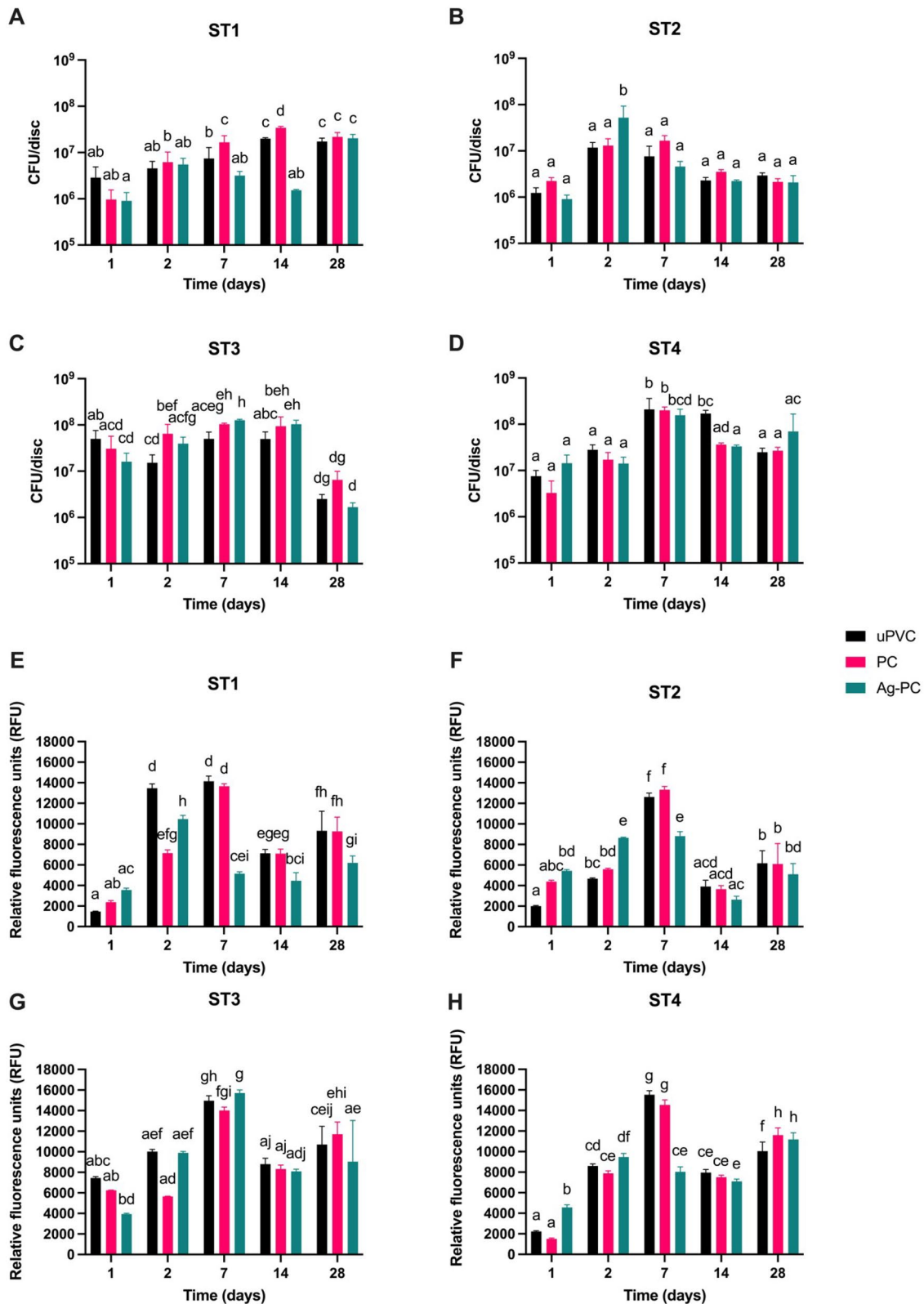


**Figure 10.** Antibiofilm efficacy of surfaces following *in situ* testing in real-world sink traps under normal usage and conditions. Biofilm on disks was quantified by colony counts following detachment (A–D) and by the resazurin assay without biofilm detachment (E–H). uPVC, unplasticized polyvinyl chloride; PC, pipe cement coating; Ag-PC, silver-pipe cement coating. Data presented as means  $\pm$  S.D., from one experimental run. Different letters indicate significant differences at  $p < 0.05$  for all comparisons between the test groups across endpoints (two-way ANOVA followed by Tukey's *post hoc* test).

## 4. Discussion

In this study, a novel nanocomposite was prepared by successfully dispersing Ag NPs in a matrix made of an inexpensive commercially available pipe cement product. This Ag nanocomposite was then applied to the surface of uPVC specimens as a thin film, before it was fully characterized, and its antibacterial properties tested. This Ag nanocoating was envisaged for application to the surface of polymers commonly used in wastewater plumbing systems – chiefly sink traps – in hospitals and with the aim to reduce nosocomial infections, which often originate in these locations. The Ag nanocoating was confirmed to be highly stable both in water and culture media, in line with previous studies (Besinis et al. 2017; Meran et al. 2018; Stebounova et al. 2011). The Ag-PC nanocoating was found to have strong antibiofilm and antiplanktonic activity *in vitro* when tested against three representative bacterial species in monoculture, and bacterial communities derived from sink traps located in hospital and university buildings. These communities were analyzed using targeted 16S rRNA gene sequencing to characterize the ‘microbiome’ present. Further *in situ* experiments demonstrated strong medium-term antibiofilm activity for the Ag-PC nanocoatings in a benchtop sink trap rig over 11 days but with more variable findings in real-world sink traps in the university buildings, where protection was either not evident or lasted up to 28 days.

### 4.1. Use of 16S rRNA gene sequencing to characterize sink trap bacterial communities

Despite the fact that hospital sink traps have historically been reported to contain a dense bacterial community with  $10^6$ – $10^{10}$  CFU mL<sup>-1</sup> of predominantly Gram-negative rods (Döring et al. 1991), and a variety of bacteria have been isolated from hospital sinks (Lowe et al. 2012; Landelle et al. 2013; Loveday et al. 2014; Regev-Yochay et al. 2018; Volling et al. 2020; Franco et al. 2020; Jamal et al. 2020; De Geyter et al. 2021; Nurjadi et al. 2021; Kehl et al. 2022), little previous work has been published applying 16S rRNA gene sequencing to hospital sink trap communities. It is widely acknowledged that culture-dependent methods do not reflect the true microbial diversity present in natural or built environments (Schleifer 2004; Donachie, Foster, and Brown 2007).

Next generation sequencing methods based on the 16S rRNA gene have previously been applied

to characterize biofilms from domestic shower hoses, finding that culture-based methods detected <1% of the flora actually present (Moat et al. 2016). Sequencing especially helps in detecting difficult-to-culture organisms, which may be predominant members of the microbial community (Chan, Naphtali, and Schellhorn 2019; Boers, Jansen, and Hays 2019). To the best of our knowledge, very few previously published studies have performed 16S rRNA gene sequencing surveys of hospital sink traps. One such study sampled two sink traps from patient rooms in a hospital and sequenced the 16S V4 region (Burgos-Garay et al. 2021), while another sampled sinks (although the authors did not specify which part of the sink) and other surfaces across three hospitals, sequencing the 16S V3–4 region (Yano et al. 2017). The use of the Oxford Nanopore Technologies MinION platform for long-read 16S rRNA gene sequencing has been applied as proof-of-concept on hospital sink trap samples, with a proposal to introduce more widespread ‘point-of-care’ characterization of microorganisms dwelling in wastewater plumbing systems (Butler and Upton 2023). Other related studies (which did not employ 16S rRNA gene amplicon surveys) include use of culturomics to explore viable microbiota in hospital drain samples (Pirzadian et al. 2020) and an investigation of surface sanitization protocols in the hospital environment, including the ceramic part of sinks (Klassert et al. 2022). There has also been a 16S rRNA gene sequencing study of a communal sink trap on a university campus, describing taxa at the family level (Withey et al. 2021), and an investigation of domestic sink traps (McBain et al. 2003).

Our findings showing that hospital sink traps were dominated by commonly pathogenic genera such as *Pseudomonas*, *Citrobacter*, *Serratia*, *Enterobacter* and *Clostridioides* (Figure 6) are consistent with previous reports in the literature, though these were mostly culture-based studies (Regev-Yochay et al. 2018; Volling et al. 2020; Franco et al. 2020; Jamal et al. 2020; De Geyter et al. 2021; Nurjadi et al. 2021; Kehl et al. 2022; Butler and Upton 2023; Wolf et al. 2014; Zhou et al. 2016; Decraene et al. 2018; de Jonge et al. 2019; Kotay et al. 2020; Park et al. 2020; Jamal et al. 2021). The findings emphasize the need to identify new solutions to address the presence of potentially pathogenic bacteria in sink traps in clinical areas. We also characterized the microbiome of university building toilet (i.e., non-clinical) handwashing sink traps, demonstrating predominance of environmental bacteria including *Citrobacter*, *Desulfovibrio*, *Dethiosulfovibrio*, *Kluyvera*, *Anaerophaga*, *Bacillus*, and

*Staphylococcus* (Figure 8). *Staphylococcus* and *Bacillus* have previously been identified in domestic sink traps (McBain et al. 2003), while *Kluyvera* has previously been identified from a hospital sink (Liu et al. 2020). The contrasting data further demonstrate that wastewater plumbing systems in clinical areas are more likely to be colonized with (opportunistic) pathogens than wastewater plumbing systems in other locations. Larger scale studies of this nature may indicate that interventions targeting sink trap microbial communities could be effectively deployed strategically, rather than used in all settings.

Particularly for the university building sink trap characterization, sequencing of the 16S rRNA gene targeting the V3–4 region revealed significantly higher diversity than was revealed by the V4–5 region. Table S1 indicates a large number of genera ( $n=76$ ) were detected by V3–4 sequencing but not by V4–5 sequencing, even though the same sample was used. This demonstrates that primer pair selection can significantly skew the analysis of complex microbial communities, potentially leading to misrepresentation of community composition or lack of resolution to detect certain taxa. The reliance of amplicon sequencing on PCR introduces a degree of bias due to the fact that DNA from some bacteria is amplified more efficiently during PCR (amplification bias) than DNA from others (Silverman et al. 2021; Kennedy et al. 2014) and the ability to lyse different bacteria may vary (extraction bias) leading to differences in the contribution of bacteria from different genera to the ‘pool’ of DNA available for sequencing (Salonen et al. 2010; Brooks et al. 2015; Gill et al. 2016). It is important for researchers to define the optimal gene regions to amplify and sequence, as this varies based on the environment being studied and can significantly affect the results (Yu et al. 2008; Klindworth et al. 2013; Yang, Wang, and Qian 2016; Bukin et al. 2019), as has also been demonstrated here.

#### 4.2. Characterization of coating surface roughness and topography

The surface roughness was expressed quantitatively by  $R_a$  and  $R_z$  measurements (Table 1), and further illustrated by representative 3D topography images (Figure 2). The surface of uncoated uPVC was flat and smooth, but application of the Ag-PC nanocoatings increased the surface roughness moderately. Grinding of the nanocoatings to expose the Ag NPs increased the surface roughness twofold, mainly due to the scratches and grooves introduced

during the process. Additional analysis by SEM confirmed the above findings and offered a clear presentation of the surface nanotopography for the different control and test groups (Figure 3A–E).

Surface roughness and topography are known to be key modulating factors in bacterial adhesion and biofilm formation, with an increase in roughness generally leading to greater ability for adherence due to increased specific surface area, as well as protection from shear forces and abrasion against other surfaces (see review by Crawford et al. (2012)). There is conventional wisdom that surfaces intended to minimize bacterial attachment should be designed to be smooth (Mitik-Dineva et al. 2008; Xing et al. 2015), however there is further ongoing debate concerning how smooth a surface must be to lend true anti-adhesion properties, as even nanoscale surface roughness can be exploited by bacteria to provide a platform for attachment (Mitik-Dineva et al. 2008). In addition, bacterial appendages such as flagella are able to facilitate attachment of apparently smooth surfaces by exploring surface ‘hummocks and hollows’ smaller than the bacteria themselves (Friedlander et al. 2013). In this study, while the uncoated uPVC appeared to be the smoothest compared to the alternative surfaces, biofilm formation clearly occurred as shown by the uPVC controls in Figures 5, 7, 9 and 10, reflecting common biofilm formation on polymer surfaces in wastewater plumbing systems. The surface roughness of the nanocoatings described here was not intentionally designed, rather the data are presented for the sake of characterization. The grinding process introduced significant additional roughness but was deemed necessary to ‘activate’ the nanocoating, presumably by exposing Ag NPs which were otherwise embedded within the pipe cement matrix.

EDS analysis confirmed the elemental composition of the different surfaces and coatings, with Cl, Si, Ca, Ti, and Ag being the main elements detected (Figure 3F–H). The strong signal of Cl detected was from the uPVC ( $(C_2H_3Cl)_n$ ) disks used as substrates. The presence of Si can be explained by the use of silicon carbide paper for the grinding process. Ti and Ca were only detected in the uPVC control specimens (Figure 3F). Titanium dioxide ( $TiO_2$ ) is commonly added to uPVC to protect against ultraviolet light degradation and to give a bright white color (Burn 1992; Gao, Bolt, and Feng 2008). Similarly, Ca (in the form of  $CaCO_3$ ) is added to uPVC to increase its mechanical strength (Luo and Pan 2021). The grinding process did not seem to increase the amount of Ag detected by EDS and the

backscattered images showed clusters of Ag NPs both in the unground and ground Ag-PC nanocoatings (Figure 3I,J). However, that was not a surprise since the information depth of the backscattered electron signal can be up to a few microns below the surface (Pearce and Nelson 1989) and therefore the Ag NPs shown in the backscattered SEM images were located at different depths within the pipe cement matrix. Backscattered electron imaging was employed here as a tool to confirm the presence of Ag NPs in the coatings as well as illustrate the particle distribution in the matrix, rather than verifying whether Ag NPs were exposed to the surface following the grinding process. Once Ag nanocoatings were applied to the uPVC substrates, there was some precipitation of the Ag NPs during the few minutes it took for the pipe cement to start setting. A pilot study was conducted, which showed that unground Ag nanocoatings had no antibacterial properties (data not shown). This could only be explained by absence or limited presence of Ag NPs on the very surface of the coatings and lack of bioavailability of those NPs that had precipitated within the pipe cement. Surface grinding exposed a sufficient amount of evenly distributed Ag NPs, previously embedded within the matrix, and resulted in strong antibacterial and antibiofilm performance (Figures 5, 7 and 9).

#### 4.3. Nanocoating stability

There was negligible Ag release from the Ag-PC specimens during the 24 h dialysis study (less than 0.003% material loss in Milli-Q water; Figure 4). The amount of ionic Ag leaching from the Ag-PC nanocoatings when specimens were exposed to 1% LB broth in the 24-well microplates during the exposure studies was comparatively higher, ranging from 1.499 to 2.048  $\mu\text{g}$ . These amounts corresponded to a 31-fold, 24-fold and 32-fold increase in Ag release for the Ag-PC specimens immersed in LB inoculated with *P. aeruginosa*, *A. baumannii* or *E. faecalis* in LB, respectively, compared to the dialysis study in ultrapure water. Despite that increase, the Ag release remained very limited (0.075–0.102%).

Besinis et al. (2017) have also reported very low dissolution of Ag from nanocoatings applied to titanium alloy medical implants (<0.07%), while Meran et al. (2018) found that loss of Ag as a result of dissolution from Ag nanocoatings applied to silicone maxillofacial prostheses was at levels below the detection limit of the ICP-OES instrument. Stebounova et al. (2011) also showed very limited

dissolution of nanosilver in simulated biological fluids over 24 h (<0.1%), which matches the findings of the current study for LB broth. It has previously been suggested that Ag dissolution remains reduced in physiological saline compared to ultrapure water due to the formation of a sparingly soluble AgCl precipitate in the presence of millimolar concentrations of chloride ions (Besinis et al., 2014b; Salaie et al. 2020). While this point cannot be reinforced by the data presented here, it should be noted that our assessment of Ag release in dilute bacteriological media (1% LB) was conducted during bacterial exposure experiments, not as part of a controlled dialysis experiment as was conducted with ultrapure water. Certain factors aside from media type – chiefly temperature (37°C versus room temperature), presence of bacteria, and total liquid volume (1.5 mL versus 500 mL) – differed between the assay methodologies and therefore a direct comparison should be made cautiously. Far greater Ag NP dissolution in biological media compared to inorganic salt solutions has previously been reported (Zook et al. 2011). In another study, Salaie et al. (2020) reported almost 200-fold greater Ag dissolution when nanocoatings were immersed in Dulbecco's Modified Eagle's medium (DMEM) with fetal bovine serum (FBS) compared to DMEM without FBS, indicating that the proteins in FBS may enhance Ag release. This effect has also been reported with TiO<sub>2</sub> NPs (Shi et al. 2012). While FBS was not used in this study, there are some commonalities with LB, such as the presence of macromolecules including proteins. Our dilution of LB to 1%, while maintaining osmotic balance, resulted in a composition of 0.1 g L<sup>-1</sup> tryptone, 0.05 g L<sup>-1</sup> yeast extract, and 10 g L<sup>-1</sup> NaCl. It is possible that the proteins present in the 1% LB provided -SH groups on amino acids and proteins for Ag<sup>+</sup> binding while the colloidal structure of proteins could have provided steric hindrance, entrapping AgCl particulates (Loza et al. 2014; Lead et al. 2018). This may have accounted for some of the increase in Ag release. In addition, the raised temperature in plate-based assays compared to the dialysis assay (37°C versus room temperature) may have accelerated Ag NP dissolution (Steinmetz et al. 2020). Finally, the presence of bacterial metabolites may have further driven the increase in Ag release, although there is little mention of this in the available literature since the majority of studies describe how Ag NPs affect bacteria, but not *vice versa*.

The sonication method that was employed to liberate biofilm-derived cells from the surfaces of



the different test groups for the purposes of enumeration, no matter how mild, posed a risk of causing damage to the nanocoatings. Therefore, the Ag release as a result of sonication was quantified to confirm that the integrity of the Ag-PC nanocoatings was not compromised, which also served as an additional measure of their stability. The extent of Ag release in saline did not exceed 0.038% of the total amount of Ag available in the nanocoatings for any of the exposures studies, demonstrating that the Ag-PC nanocoatings were highly stable and resilient. The Ag nanocoatings presented here were 6-fold more resilient to sonication when compared to a previous study by Besinis et al. (2017) who reported up to 0.23% metal release from pure Ag nanocoatings applied to titanium alloy substrates. The increased stability of the Ag-PC nanocoatings was most likely due to the protective action of the pipe cement matrix.

The relatively low dissolution of Ag NPs when applied as nanocoatings to the surface of medical implants and maxillofacial prostheses can justify their use *in vivo*, since low levels of Ag release suggest low levels of exposure of the surrounding tissues and therefore potentially low levels of resulting inflammation and toxicity (Meran et al. 2018; Stebounova et al. 2011). For the purposes of the Ag nanocoating described here, low levels of Ag release are highly desirable to alleviate concerns over Ag escaping into the wastewater plumbing systems and subsequently causing toxicity to the aquatic environment (Salaie et al. 2020; Lead et al. 2018). Meanwhile, achieving a low controlled dissolution also suggests increased longevity of the antibacterial and antibiofilm activity of the nanocoating since the Ag NPs available on the surface of the coating will not be rapidly depleted. The microbes in this study were killed by Ag NPs, in conditions where release of free Ag<sup>+</sup> in the media remained very low. One possible mode of action is direct contact of the particles with the bacterial cell wall as previously described by Besinis et al. (2014b).

#### **4.4. Antibiofilm and antiplanktonic activity of nanocoatings *in vitro* against three representative bacterial species and a hospital sink trap bacterial community**

Overall, the Ag-PC nanocoating exhibited significant antibiofilm properties resulting in log<sub>10</sub> reductions of 2.9–7.2 in culturable biofilm-derived cells (equivalent to reductions of 99.82–100%) compared to the uncoated uPVC controls (Figure 5). The Ag nanocoating was also found to be highly potent exhibiting

reproducible reductions in the viability of planktonic bacteria, with log<sub>10</sub> reductions of 2.4–4.5 (equivalent to reductions of 99.59–99.99%) compared to wells containing uncoated uPVC disks. Results showing antibiofilm activity were confirmed in all cases using a regrowth assay in broth and through application of the resazurin assay. All three representative bacterial species and the hospital sink trap bacteria were able to form biofilms on the uncoated uPVC and PC disks, with consistent bacterial numbers of 10<sup>6</sup>–10<sup>7</sup> CFU/disk measured by enumeration following detachment of biofilms by sonication. Any differences in the numbers of cultured biofilm-derived bacteria between the uPVC and PC groups were either not significant (e.g., for *P. aeruginosa* and *A. baumannii*; Figure 5A,B), or very small (e.g., log<sub>10</sub> reduction of 0.15 for *E. faecalis* biofilm formed on PC surfaces; Figure 5C) indicating that pipe cement had no effect on biofilm development.

The use of dilute (1% LB broth) rather than full strength bacteriological media was intended to more closely mimic the nutrient-poor conditions experienced in wastewater plumbing systems. Previous studies have utilized minimal media such as Reasoner's 2A broth to simulate sink trap conditions (Kotay et al. 2020; Garratt et al. 2021; Butler et al. 2022), and here we propose that the use of 1% LB broth (with care taken to maintain appropriate osmotic balance) achieves similar aims. The use of a defined minimal medium is favorable as it ensures consistency to controlled experiments over what could have been achieved by use of, for example, autoclaved tap water or autoclaved sink trap contents. However, there is no perfect laboratory model to mimic real-life sink traps or wastewater plumbing systems because use of the sink, and the disposal of liquids and solids, will result in variable nutrient conditions (Garratt et al. 2021; Grabowski et al. 2018).

#### **4.5. Antibiofilm activity and discord between laboratory-based *in vitro* and real-world *in situ* experiments**

The main objective of developing the Ag-PC nanocoating was to inhibit biofilm formation, as it is well-established that once biofilms form they harbor pathogens, resist disinfection (Flemming et al. 2016; Ledwoch et al. 2020) and provide a platform for horizontal transfer of antibiotic resistance genes (Hennequin et al. 2012; Savage, Chopra, and O'Neill 2013). In fact, disk exposure experiments performed *in vitro* under controlled laboratory conditions using a panel of nosocomial pathogens, a hospital sink

trap bacterial community (Figure 5), and a university building sink trap bacterial community (Figure 9) showed that Ag-PC nanocoatings had a very strong antibiofilm performance, inhibiting biofilm development by at least 99.82%. However, when disks were placed in real-world sink traps, data were less consistent, showing limited or medium-term antibiofilm performance (e.g., significantly reduced biofilm development on Ag-PC disks between 7 and 28 days for ST1; on day 7 for ST2 and ST4), or in the case of ST3 no treatment effect at all (Figure 9). The fact that Ag-PC nanocoatings did confer antibacterial activity against the bacteria present in the sink traps *in vitro*, but these findings were not equally confirmed by the *in situ* experiments, suggests it was due to other confounding factors. When disks were collected from sink traps during the *in situ* experiments, a build-up of physical contaminants was visually evident on the disk surfaces, fully covering the applied nanocoatings. We suggest that this layer of foreign matter was the main reason for the limited antibiofilm efficacy of the Ag-PC nanocoatings. The formation of a conditioning film is well-documented in aqueous conditions, where biomolecules adsorbing to surfaces modify their surface properties, paving the way for microbial attachment and biofilm formation (Bhagwat et al. 2021; Marsh et al. 2016; Rummel et al. 2021; Francius et al. 2017). Sink traps contain a wide variety of microscopic and macroscopic 'debris', which may include organic matter from drinking water (Francius et al. 2017), dead or sloughed skin cells, hair and dirt from handwashing, or less frequently a variety of substances such as discarded food and drink (Balm et al. 2013), that may introduce unexpected variables. Handwashing sink activities have previously been characterized in a hospital intensive care unit, demonstrating that handwashing represented only 4% of total behaviors, with further analysis indicating 56 activities which could introduce nutritional substances for microbes into the sink (Grabowski et al. 2018). It is therefore likely that these substances, along with any dead bacteria, would form a film on the surface of the Ag-PC nanocoatings rendering Ag NPs not bioavailable, and thus reducing or even masking their antibiofilm effect. There is currently little information in the published literature concerning the impact of the variety of inert debris found in wastewater on biofilm formation and fouling of surfaces, but it is highly likely that any future work to develop antimicrobial nanocoatings for such challenging environments would require additional mechanisms to reduce that impact.

There are various examples in the literature of previous studies that have sought to simulate the conditions in real-world sink traps, for example by transplanting a hospital sink trap into an automated model sink drain system to study the effect of long-term exposure of sink trap bacteria to the disinfectant octenidine (Garratt et al. 2021). The laboratory model system consisted of 12 individual sinks with associated pipework and bottle-style sink traps built to simulate a clinical setting (Aranega-Bou et al. 2019). Other work has employed an artificial 'sink gallery' composed of five identical adjacent sinks linked to a common drainpipe to study *Escherichia coli* dispersal from handwashing sink traps during use (Kotay et al. 2017) and the dynamics of carbapenemase-producing Enterobacterales in response to nutrient exposure (Kotay et al. 2020). However, these studies primarily focused on modeling bacterial dispersal from sink traps, persistence in biofilms, and the effect of nutrient and disinfectant exposure on persistence and antimicrobial resistance, rather than attempting to test antimicrobial strategies *in situ*, as was performed in our work. Formation of a conditioning film or deposition of other inhibitory compounds is expected to be an issue for any antimicrobial nanocoating or surface that relies on direct exposure of bacteria to an active substance in order to prevent biofilm development. This needs to be considered as a limiting factor affecting not just wastewater plumbing systems applications, but also any type of antimicrobial nanocoatings developed for other settings in medicine such as medical implants, prostheses and biomaterials. Any future research endeavors within the realm of developing antimicrobial coatings should always seek to include realistic, preferably 'real-world' or '*in situ*' testing, because the performance of those coatings cannot otherwise be confidently verified.

## 5. Conclusion

The development of an Ag nanocomposite applied as a coating rendered the surface of uPVC highly antibacterial against the representative nosocomial pathogens *P. aeruginosa*, *A. baumannii*, and *E. faecalis*, as well as against polymicrobial communities from sink traps in a university building and a hospital. The strong antibacterial activity of the Ag nanocoating was expressed both as inhibition of bacterial growth in the surrounding media and as reduction of biofilm formation on the coated surfaces *in vitro*. The nanocoating was found to have increased surface roughness compared to the uncoated uPVC control and

was highly stable in the conditions tested. Sequencing of 16S rRNA gene amplicons was used to characterize the bacterial taxa present in university and hospital sink traps, identifying a number of known nosocomial pathogens. Data presented indicate that the developed nanocoating was effective against clinically-relevant bacteria in these consortia. More realistic experimental conditions, based on a novel benchtop sink trap model system, indicated significant antibiofilm efficacy up to 11 days but not after 25 days. However, antibiofilm efficacy in real-world sink traps indicated no clear overall effect despite examples of 28-day antibiofilm activity in some cases. It is suggested that the complex real-world conditions encountered led to formation of a conditioning film that masked the antibacterial performance of the Ag nanocoating. This has wider relevance to antimicrobial nanocoating development across fields including medicine, dentistry, and plumbing systems in healthcare settings.

## Acknowledgements

The assistance by Estates and Research & Development staff at University Hospitals Plymouth NHS Trust for facilitating the collection of samples is gratefully acknowledged. The authors thank Dr Paul Waines for advice and support in conducting experiments, and Mr Peter Brennan and Mr Simon Knight for facilitating experiments and sample collection at the University of Plymouth. The authors thank Mr Glenn Harper at Plymouth Electron Microscopy Centre for his assistance with SEM and EDS, and Dr Robert Clough at the Analytical Research Facility, University of Plymouth, for his assistance with ICP-OES and ICP-MS.

## Authors' contributions

Conceptualization: JB, MU and AB; Data curation: JB and AB; Formal analysis: JB and AB; Funding acquisition: AB; Investigation: JB, SM and LJ; Methodology: JB, SM, MU and AB; Project administration: MU and AB; Resources: LJ, MU and AB; Supervision: MU and AB; Validation: JB and AB; Visualization: JB, SM and AB; Writing – original draft: JB; Writing – review & editing: JB, SM, LJ, MU and AB.

## Disclosure statement

No potential conflict of interest was reported by the author(s).

## Funding

This work was funded by a research grant awarded to Dr Alexandros Besinis by the School of Engineering, Computing and Mathematics at the University of Plymouth. James Butler received a full PhD scholarship through this grant.

## Data availability statement

The data that support the findings of this study are available from the corresponding author, Dr Alexandros Besinis, upon reasonable request.

## References

- Allaker, R. P. 2010. "The Use of Nanoparticles to Control Oral Biofilm Formation." *Journal of Dental Research* 89 (11): 1175–1186. <https://doi.org/10.1177/0022034510377794>.
- Aranega-Bou, P., R. P. George, N. Q. Verlander, S. Paton, A. Bennett, G. Moore, Z. Aiken, et al. 2019. "Carbapenem-Resistant Enterobacteriaceae Dispersal from Sinks is Linked to Drain Position and Drainage Rates in a Laboratory Model System." *The Journal of Hospital Infection* 102 (1): 63–69. <https://doi.org/10.1016/j.jhin.2018.12.007>.
- Armitage, D. W., K. L. Gallagher, N. D. Youngblut, D. H. Buckley, and S. H. Zinder. 2012. "Millimeter-Scale Patterns of Phylogenetic and Trait Diversity in a Salt Marsh Microbial Mat." *Frontiers in Microbiology* 3: 293–293. <https://doi.org/10.3389/fmicb.2012.00293>.
- Balm, M. N., S. Salmon, R. Jureen, C. Teo, R. Mahdi, T. Seetoh, J. T. Teo, R. T. Lin, and D. A. Fisher. 2013. "Bad Design, Bad Practices, Bad Bugs: frustrations in Controlling an Outbreak of Elizabethkingia meningoseptica in Intensive Care Units." *The Journal of Hospital Infection* 85 (2): 134–140. <https://doi.org/10.1016/j.jhin.2013.05.012>.
- Besinis, A., S. D. Hadi, H. R. Le, C. Tredwin, and R. D. Handy. 2017. "Antibacterial Activity and Biofilm Inhibition by Surface Modified Titanium Alloy Medical Implants following Application of Silver, Titanium Dioxide and Hydroxyapatite Nanocoatings." *Nanotoxicology* 11 (3): 327–338. <https://doi.org/10.1080/17435390.2017.1299890>.
- Besinis, A., T. De Peralta, and R. D. Handy. 2014a. "Inhibition of Biofilm Formation and Antibacterial Properties of a Silver Nano-Coating on Human Dentine." *Nanotoxicology* 8 (7): 745–754. <https://doi.org/10.3109/17435390.2013.825343>.
- Besinis, A., T. De Peralta, and R. D. Handy. 2014b. "The Antibacterial Effects of Silver, Titanium Dioxide and Silica Dioxide Nanoparticles Compared to the Dental Disinfectant Chlorhexidine on *Streptococcus mutans* Using a Suite of Bioassays." *Nanotoxicology* 8 (1): 1–16. <https://doi.org/10.3109/17435390.2012.742935>.
- Bhagwat, Geetika, Wayne O'Connor, Ian Grainge, and Thava Palanisami. 2021. "Understanding the Fundamental Basis for Biofilm Formation on Plastic Surfaces: Role of Conditioning Films." *Frontiers in Microbiology* 12: 687118. <https://doi.org/10.3389/fmicb.2021.687118>.
- Boers, S. A., R. Jansen, and J. P. Hays. 2019. "Understanding and Overcoming the Pitfalls and Biases of Next-Generation Sequencing (NGS) Methods for Use in the Routine Clinical Microbiological Diagnostic Laboratory." *European Journal of Clinical Microbiology & Infectious Diseases* 38 (6): 1059–1070. <https://doi.org/10.1007/s10096-019-03520-3>.
- Brooks, J. Paul, David J. Edwards, Michael D. Harwich, Maria C. Rivera, Jennifer M. Fettweis, Myrna G. Serrano, Robert A. Reris, et al. 2015. "The Truth about Metagenomics: Quantifying and Counteracting Bias in 16S rRNA Studies." *BMC Microbiology* 15 (1): 66. <https://doi.org/10.1186/s12866-015-0351-6>.

- Bukin, Y. S., Y. P. Galachyants, I. V. Morozov, S. V. Bukin, A. S. Zakharenko, and T. I. Zemskaya. 2019. "The Effect of 16S rRNA Region Choice on Bacterial Community Metabarcoding Results." *Scientific Data* 6 (1): 190007. <https://doi.org/10.1038/sdata.2019.7>.
- Burgos-Garay, M., C. Ganim, T. J. B. de Man, T. Davy, A. J. Mathers, S. Kotay, J. Daniels, K. A. Perry, E. Breaker, and R. M. Donlan. 2021. "Colonization of Carbapenem-Resistant *Klebsiella pneumoniae* in a Sink-Drain Model Biofilm System." *Infection Control and Hospital Epidemiology* 42 (6): 722–730. <https://doi.org/10.1017/ice.2020.1287>.
- Burn, L. S. 1992. "The Influence of Titanium Dioxide on the Durability of uPVC Pipe." *Polymer Degradation and Stability* 36 (2): 155–167. [https://doi.org/10.1016/0141-3910\(92\)90152-U](https://doi.org/10.1016/0141-3910(92)90152-U).
- Butler, J., and M. Upton. 2023. "What's Really down the Hospital Plughole?" *The Journal of Hospital Infection* 138: 92–93. <https://doi.org/10.1016/j.jhin.2023.04.005>.
- Butler, J., R. D. Handy, M. Upton, and A. Besinis. 2023. "Review of Antimicrobial Nanocoatings in Medicine and Dentistry: Mechanisms of Action, Biocompatibility Performance, Safety, and Benefits Compared to Antibiotics." *ACS Nano* 17 (8): 7064–7092. <https://doi.org/10.1021/acsnano.2c12488>.
- Butler, J., S. D. Kelly, K. J. Muddiman, A. Besinis, and M. Upton. 2022. "Hospital Sink Traps as a Potential Source of the Emerging Multidrug-Resistant Pathogen *Cupriavidus pauculus*: characterization and Draft Genome Sequence of Strain MF1." *Journal of Medical Microbiology* 71 (2): 001501. <https://doi.org/10.1099/jmm.0.001501>.
- Caporaso, J. G., C. L. Lauber, W. A. Walters, D. Berg-Lyons, C. A. Lozupone, P. J. Turnbaugh, N. Fierer, and R. Knight. 2011. "Global Patterns of 16S rRNA Diversity at a Depth of Millions of Sequences per Sample." *Proceedings of the National Academy of Sciences of the United States of America* 108 (Suppl 1): 4516–4522. <https://doi.org/10.1073/pnas.1000080107>.
- Cassini, Alessandro, Diamantis Plachouras, Tim Eckmanns, Muna Abu Sin, Hans-Peter Blank, Tanja Ducombe, Sebastian Haller, et al. 2016. "Burden of Six Healthcare-Associated Infections on European Population Health: Estimating Incidence-Based Disability-Adjusted Life Years through a Population Prevalence-Based Modelling Study." *PLoS Medicine* 13 (10): e1002150. <https://doi.org/10.1371/journal.pmed.1002150>.
- CDC. 2022. "COVID-19: U.S. Impact on Antimicrobial Resistance, Special Report 2022." <https://doi.org/10.15620/cdc:117915>.
- Chan, A. W., J. Naphtali, and H. E. Schellhorn. 2019. "High-Throughput DNA Sequencing Technologies for Water and Wastewater Analysis." *Science Progress* 102 (4): 351–376. <https://doi.org/10.1177/0036850419881855>.
- Chen, Chen, Xiaolei Song, Weixia Wei, Huanzi Zhong, Juanjuan Dai, Zhou Lan, Fei Li, et al. 2017. "The Microbiota Continuum along the Female Reproductive Tract and Its Relation to Uterine-Related Diseases." *Nature Communications* 8 (1): 875. <https://doi.org/10.1038/s41467-017-00901-0>.
- Crawford, R. J., H. K. Webb, V. K. Truong, J. Hasan, and E. P. Ivanova. 2012. "Surface Topographical Factors Influencing Bacterial Attachment." *Advances in Colloid and Interface Science* 179–182: 142–149. <https://doi.org/10.1016/j.cis.2012.06.015>.
- Darouiche, R. O. 2001. "Device-Associated Infections: A Macroproblem That Starts with Microadherence." *Clinical Infectious Diseases* 33 (9): 1567–1572. <https://doi.org/10.1086/323130>.
- De Geyter, D., R. Vanstokstraeten, F. Crombé, J. Tommassen, I. Wybo, and D. Piérard. 2021. "Sink Drains as Reservoirs of VIM-2 Metallo- $\beta$ -Lactamase-Producing *Pseudomonas aeruginosa* in a Belgian Intensive Care Unit: Relation to Patients Investigated by Whole-Genome Sequencing." *The Journal of Hospital Infection* 115: 75–82. <https://doi.org/10.1016/j.jhin.2021.05.010>.
- de Jonge, E., M. G. J. de Boer, E. H. R. van Essen, H. C. M. Dogterom-Ballering, and K. E. Veldkamp. 2019. "Effects of a Disinfection Device on Colonization of Sink Drains and Patients during a Prolonged Outbreak of Multidrug-Resistant *Pseudomonas aeruginosa* in an Intensive Care Unit." *The Journal of Hospital Infection* 102 (1): 70–74. <https://doi.org/10.1016/j.jhin.2019.01.003>.
- Decraene, V., H. T. T. Phan, R. George, D. H. Wyllie, O. Akinremi, Z. Aiken, P. Cleary, et al. 2018. "A Large, Refractory Nosocomial Outbreak of *Klebsiella pneumoniae* Carbapenemase-Producing *Escherichia coli* Demonstrates Carbapenemase Gene Outbreaks Involving Sink Sites Require Novel Approaches to Infection Control." *Antimicrobial Agents and Chemotherapy* 62 (12): e01689–01618. <https://doi.org/10.1128/AAC.01689-18>.
- Donachie, S. P., J. S. Foster, and M. V. Brown. 2007. "Culture Clash: challenging the Dogma of Microbial Diversity." *The ISME Journal* 1 (2): 97–99. <https://doi.org/10.1038/ismej.2007.22>.
- Döring, G., M. Ulrich, W. Müller, J. Bitzer, L. Schmidt-Koenig, L. Münst, H. Grupp, C. Wolz, M. Stern, and K. Botzenhart. 1991. "Generation of *Pseudomonas aeruginosa* Aerosols during Handwashing from Contaminated Sink Drains, Transmission to Hands of Hospital Personnel, and Its Prevention by Use of a New Heating Device." *Zentralblatt für Hygiene und Umweltmedizin = International journal of hygiene and environmental medicine* 191 (5-6): 494–505.
- Edwardson, C. F., and J. T. Hollibaugh. 2018. "Composition and Activity of Microbial Communities along the Redox Gradient of an Alkaline, Hypersaline, Lake." *Frontiers in Microbiology* 9: 14–14. <https://doi.org/10.3389/fmicb.2018.00014>.
- Flemming, H.-C., J. Wingender, U. Szewzyk, P. Steinberg, S. A. Rice, and S. Kjelleberg. 2016. "Biofilms: An Emergent Form of Bacterial Life." *Nature Reviews. Microbiology* 14 (9): 563–575. <https://doi.org/10.1038/nrmicro.2016.94>.
- Francius, G., R. El Zein, L. Mathieu, F. Gosselin, A. Maul, and J.-C. Block. 2017. "Nano-Exploration of Organic Conditioning Film Formed on Polymeric Surfaces Exposed to Drinking Water." *Water Research* 109: 155–163. <https://doi.org/10.1016/j.watres.2016.11.038>.
- Franco, L. C., W. Tanner, C. Ganim, T. Davy, J. Edwards, and R. Donlan. 2020. "A Microbiological Survey of Handwashing Sinks in the Hospital Built Environment Reveals Differences in Patient Room and Healthcare Personnel Sinks." *Scientific Reports* 10 (1): 8234. <https://doi.org/10.1038/s41598-020-65052-7>.
- Friedlander, R. S., H. Vlamakis, P. Kim, M. Khan, R. Kolter, and J. Aizenberg. 2013. "Bacterial Flagella Explore Microscale Hummocks and Hollows to Increase Adhesion." *Proceedings of the National Academy of Sciences of the United States of America* 110 (14): 5624–5629. <https://doi.org/10.1073/pnas.1219662110>.
- Gao, A. X., J. D. Bolt, and A. A. Feng. 2008. "Role of Titanium Dioxide Pigments in Outdoor Weathering of Rigid PVC." *Plastics, Rubber and Composites* 37 (9-10): 397–402. <https://doi.org/10.1179/174328908X356545>.



- Garratt, I., P. Aranega-Bou, J. M. Sutton, G. Moore, M. E. Wand, and A. J. McBain. 2021. "Long-Term Exposure to Octenidine in a Simulated Sink Trap Environment Results in Selection of *Pseudomonas aeruginosa*, *Citrobacter*, and *Enterobacter* Isolates with Mutations in Efflux Pump Regulators." *Applied and Environmental Microbiology* 87 (10): e00210–00221. <https://doi.org/10.1128/AEM.00210-21>.
- Gill, C., J. H. H. M. van de Wijkert, F. Blow, and A. C. Darby. 2016. "Evaluation of Lysis Methods for the Extraction of Bacterial DNA for Analysis of the Vaginal Microbiota." *PloS One* 11 (9): e0163148. <https://doi.org/10.1371/journal.pone.0163148>.
- Global and Public Health Group (Emergency Preparedness and Health Protection Policy Directorate). 2019. *Contained and Controlled: The UK's 20-Year Vision for Antimicrobial Resistance*. London: Department of Health and Social Care.
- Gormley, M., T. J. Aspray, D. A. Kelly, and C. Rodriguez-Gil. 2017. "Pathogen Cross-Transmission via Building Sanitary Plumbing Systems in a Full Scale Pilot Test-Rig." *PloS One* 12 (2): e0171556. <https://doi.org/10.1371/journal.pone.0171556>.
- Grabowski, M., J. M. Lobo, B. Gunnell, K. Enfield, R. Carpenter, L. Barnes, and A. J. Mathers. 2018. "Characterizations of Handwashing Sink Activities in a Single Hospital Medical Intensive Care Unit." *The Journal of Hospital Infection* 100 (3): e115–e122. <https://doi.org/10.1016/j.jhin.2018.04.025>.
- Guest, J. F., T. Keating, D. Gould, and N. Wigglesworth. 2020. "Modelling the Annual NHS Costs and Outcomes Attributable to Healthcare-Associated Infections in England." *BMJ Open* 10 (1): e033367. <https://doi.org/10.1136/bmjopen-2019-033367>.
- Hajar, Z., T. S. C. Mana, J. L. Cadnum, and C. J. Donskey. 2019. "Dispersal of Gram-Negative Bacilli from Contaminated Sink Drains to Cover Gowns and Hands during Hand Washing." *Infection Control and Hospital Epidemiology* 40 (4): 460–462. <https://doi.org/10.1017/ice.2019.25>.
- Halstead, F. D., J. Quick, M. Niebel, M. Garvey, N. Cumley, R. Smith, T. Neal, et al. 2021. "*Pseudomonas aeruginosa* Infection in Augmented Care: The Molecular Ecology and Transmission Dynamics in Four Large UK Hospitals." *The Journal of Hospital Infection* 111: 162–168. <https://doi.org/10.1016/j.jhin.2021.01.020>.
- Handy, R. D., F. B. Eddy, and G. Romain. 1989. "In Vitro Evidence for the Ionoregulatory Role of Rainbow Trout Mucus in Acid, Acid/Aluminium and Zinc Toxicity." *Journal of Fish Biology* 35 (5): 737–747. <https://doi.org/10.1111/j.1095-8649.1989.tb03024.x>.
- Hennequin, C., C. Aumeran, F. Robin, O. Traore, and C. Forestier. 2012. "Antibiotic Resistance and Plasmid Transfer Capacity in Biofilm Formed with a CTX-M-15-Producing *Klebsiella pneumoniae* Isolate." *The Journal of Antimicrobial Chemotherapy* 67 (9): 2123–2130. <https://doi.org/10.1093/jac/dks169>.
- Hiergeist, A., U. Reischl, and A. Gessner. 2016. "Multicenter Quality Assessment of 16S Ribosomal DNA-Sequencing for Microbiome Analyses Reveals High Inter-Center Variability." *International Journal of Medical Microbiology: IJMM* 306 (5): 334–342. <https://doi.org/10.1016/j.ijmm.2016.03.005>.
- Hota, S., Z. Hirji, K. Stockton, C. Lemieux, H. Dedier, G. Wolfaardt, and M. A. Gardam. 2009. "Outbreak of Multidrug-Resistant *Pseudomonas aeruginosa* Colonization and Infection Secondary to Imperfect Intensive Care Unit Room Design." *Infection Control and Hospital Epidemiology* 30 (1): 25–33. <https://doi.org/10.1086/592700>.
- Hugerth, Luisa W., Marcela Pereira, Yinghua Zha, Maike Seifert, Vilde Kaldhusdal, Fredrik Boulund, Maria C. Krog, et al. 2020. "Assessment of In Vitro and In Silico Protocols for Sequence-Based Characterization of the Human Vaginal Microbiome." *mSphere* 5 (6): e00448-00420. <https://doi.org/10.1128/mSphere.00448-20>.
- Jamal, A. J., L. F. Mataseje, K. A. Brown, K. Katz, J. Johnstone, M. P. Muller, V. G. Allen, et al. 2020. "Carbapenemase-Producing Enterobacterales in Hospital Drains in Southern Ontario, Canada." *The Journal of Hospital Infection* 106 (4): 820–827. <https://doi.org/10.1016/j.jhin.2020.09.007>.
- Jamal, A. J., R. Pantelidis, R. Sawicki, A. X. Li, W. Chiu, D. Morrison, J. Marshman, et al. 2021. "Standard versus Combined Chemical, Mechanical, and Heat Decontamination of Hospital Drains Harboring Carbapenemase-Producing Organisms (CPOs): A Randomized Controlled Trial." *Infection Control and Hospital Epidemiology* 42 (10): 1275–1278. <https://doi.org/10.1017/ice.2020.1384>.
- Kehl, K., A. Schallenberg, C. Szekat, C. Albert, E. Sib, M. Exner, N. Zacharias, C. Schreiber, M. Parčina, and G. Bierbaum. 2022. "Dissemination of Carbapenem Resistant Bacteria from Hospital Wastewater into the Environment." *The Science of the Total Environment* 806 (Pt 4): 151339. <https://doi.org/10.1016/j.scitotenv.2021.151339>.
- Kennedy, K., M. W. Hall, M. D. Lynch, G. Moreno-Hagelsieb, and J. D. Neufeld. 2014. "Evaluating Bias of Illumina-Based Bacterial 16S rRNA Gene Profiles." *Applied and Environmental Microbiology* 80 (18): 5717–5722. <https://doi.org/10.1128/aem.01451-14>.
- Klassert, T. E., C. Zubiria-Barrera, R. Neubert, M. Stock, A. Schneegans, M. López, D. Driesch, et al. 2022. "Comparative Analysis of Surface Sanitization Protocols on the Bacterial Community Structures in the Hospital Environment." *Clinical Microbiology and Infection* 28 (8): 1105–1112. <https://doi.org/10.1016/j.cmi.2022.02.032>.
- Klindworth, A., E. Pruesse, T. Schweer, J. Peplies, C. Quast, M. Horn, and F. O. Glöckner. 2013. "Evaluation of General 16S Ribosomal RNA Gene PCR Primers for Classical and Next-Generation Sequencing-Based Diversity Studies." *Nucleic Acids Research* 41 (1): e1–e1. <https://doi.org/10.1093/nar/gks808>.
- Koch, A. M., R. M. Nilsen, H. M. Eriksen, R. J. Cox, and S. Harthug. 2015. "Mortality Related to Hospital-Associated Infections in a Tertiary Hospital; Repeated Cross-Sectional Studies between 2004-2011." *Antimicrobial Resistance and Infection Control* 4 (1): 57. <https://doi.org/10.1186/s13756-015-0097-9>.
- Kotay, S. M., H. I. Parikh, K. Barry, H. S. Gweon, W. Guilford, J. Carroll, and A. J. Mathers. 2020. "Nutrients Influence the Dynamics of *Klebsiella pneumoniae* Carbapenemase Producing Enterobacterales in Transplanted Hospital Sinks." *Water Research* 176: 115707. <https://doi.org/10.1016/j.watres.2020.115707>.
- Kotay, S., W. Chai, W. Guilford, K. Barry, and A. J. Mathers. 2017. "Spread from the Sink to the Patient: In Situ Study Using Green Fluorescent Protein (GFP)-Expressing *Escherichia coli* to Model Bacterial Dispersion from Hand-Washing Sink-Trap Reservoirs." *Applied and Environmental Microbiology* 83 (8): e03327–03316. <https://doi.org/10.1128/AEM.03327-16>.
- Landelle, C., P. Legrand, P. Lesprit, F. Cizeau, D. Ducellier, C. Guout, P. Bréhaut, S. Soing-Altrach, E. Girou, and C.

- Brun-Buisson. 2013. "Protracted Outbreak of Multidrug-Resistant *Acinetobacter baumannii* after Intercontinental Transfer of Colonized Patients." *Infection Control and Hospital Epidemiology* 34 (2): 119–124. <https://doi.org/10.1086/669093>.
- Lead, J. R., G. E. Batley, P. J. J. Alvarez, M. N. Croteau, R. D. Handy, M. J. McLaughlin, J. D. Judy, and K. Schirmer. 2018. "Nanomaterials in the Environment: Behavior, Fate, Bioavailability, and Effects-An Updated Review." *Environmental Toxicology and Chemistry* 37 (8): 2029–2063. <https://doi.org/10.1002/etc.4147>.
- Ledwoch, K., A. Robertson, J. Lauran, P. Norville, and J. Y. Maillard. 2020. "It's a Trap! The Development of a Versatile Drain Biofilm Model and Its Susceptibility to Disinfection." *The Journal of Hospital Infection* 106 (4): 757–764. <https://doi.org/10.1016/j.jhin.2020.08.010>.
- Liu, L., Y. Feng, L. Wei, F. Qiao, and Z. Zong. 2020. "Precise Species Identification and Taxonomy Update for the Genus *Kluyvera* With Reporting *Kluyvera sichuanensis* sp. nov." *Frontiers in Microbiology* 11: 615117. <https://doi.org/10.3389/fmicb.2020.579306>.
- Loveday, H. P., J. A. Wilson, K. Kerr, R. Pitchers, J. T. Walker, and J. Browne. 2014. "Association between Healthcare Water Systems and *Pseudomonas aeruginosa* Infections: A Rapid Systematic Review." *The Journal of Hospital Infection* 86 (1): 7–15. <https://doi.org/10.1016/j.jhin.2013.09.010>.
- Lowe, Christopher, Barbara Willey, Anna O'Shaughnessy, Wayne Lee, Ming Lum, Karen Pike, Cindy Larocque, et al. 2012. "Outbreak of Extended-Spectrum  $\beta$ -Lactamase-Producing *Klebsiella oxytoca* Infections Associated with Contaminated Handwashing Sinks." *Emerging Infectious Diseases* 18 (8): 1242–1247. <https://doi.org/10.3201/eid1808.111268>.
- Loza, K., J. Diendorf, C. Sengstock, L. Ruiz-Gonzalez, J. M. Gonzalez-Calbet, M. Vallet-Regi, M. Köller, and M. Epple. 2014. "The Dissolution and Biological Effects of Silver Nanoparticles in Biological Media." *Journal of Materials Chemistry. B* 2 (12): 1634–1643. <https://doi.org/10.1039/C3TB21569E>.
- Luo, S., and S. Pan. 2021. "Numerical Study on the Effect of CaCO<sub>3</sub> Ratio on the Mechanical Properties of CaCO<sub>3</sub>/PVC Composites." *Journal of Physics: Conference Series* 1820 (1): 012140. <https://doi.org/10.1088/1742-6596/1820/1/012140>.
- Mackley, A., C. Baker, and A. Bate. 2018. "Raising Standards of Infection Prevention and Control in the NHS." House of Commons Library CDP-2018-0116.
- Marsh, P. D., T. Do, D. Beighton, and D. A. Devine. 2016. "Influence of Saliva on the Oral Microbiota." *Periodontology* 2000 70 (1): 80–92. <https://doi.org/10.1111/prd.12098>.
- McBain, A. J., R. G. Bartolo, C. E. Catrenich, D. Charbonneau, R. G. Ledder, A. H. Rickard, S. A. Symmons, and P. Gilbert. 2003. "Microbial Characterization of Biofilms in Domestic Drains and the Establishment of Stable Biofilm Microcosms." *Applied and Environmental Microbiology* 69 (1): 177–185. <https://doi.org/10.1128/AEM.69.1.177-185.2003>.
- Meran, Z., A. Besinis, T. De Peralta, and R. D. Handy. 2018. "Antifungal Properties and Biocompatibility of Silver Nanoparticle Coatings on Silicone Maxillofacial Prostheses In Vitro." *Journal of Biomedical Materials Research. Part B, Applied Biomaterials* 106 (3): 1038–1051. <https://doi.org/10.1002/jbm.b.33917>.
- Miles, A. A., S. S. Misra, and J. O. Irwin. 1938. "The Estimation of the Bactericidal Power of the Blood." *The Journal of Hygiene* 38 (6): 732–749. <https://doi.org/10.1017/s002217240001158x>.
- Mitchell, Brett G., Lisa Hall, Nicole White, Adrian G. Barnett, Kate Halton, David L. Paterson, Thomas V. Riley, et al. 2019. "An Environmental Cleaning Bundle and Health-Care-Associated Infections in Hospitals (REACH): A Multicentre, Randomised Trial." *The Lancet. Infectious Diseases* 19 (4): 410–418. [https://doi.org/10.1016/s1473-3099\(18\)30714-x](https://doi.org/10.1016/s1473-3099(18)30714-x).
- Mitik-Dineva, N., J. Wang, R. C. Mocanasu, P. R. Stoddart, R. J. Crawford, and E. P. Ivanova. 2008. "Impact of Nano-Topography on Bacterial Attachment." *Biotechnology Journal* 3 (4): 536–544. <https://doi.org/10.1002/biot.200700244>.
- Moat, J., A. Rizoulis, G. Fox, and M. Upton. 2016. "Domestic Shower Hose Biofilms Contain Fungal Species Capable of Causing Opportunistic Infection." *Journal of Water and Health* 14 (5): 727–737. <https://doi.org/10.2166/wh.2016.297>.
- Murray, C. J. L., K. S. Ikuta, F. Sharara, L. Swetschinski, G. Robles Aguilar, A. Gray, C. Han, et al. 2022. "Global Burden of Bacterial Antimicrobial Resistance in 2019: A Systematic Analysis." *Lancet* 399 (10325): 629–655. [https://doi.org/10.1016/S0140-6736\(21\)02724-0](https://doi.org/10.1016/S0140-6736(21)02724-0).
- Muyzer, G., E. C. de Waal, and A. G. Uitterlinden. 1993. "Profiling of Complex Microbial Populations by Denaturing Gradient Gel Electrophoresis Analysis of Polymerase Chain Reaction-Amplified Genes Coding for 16S rRNA." *Applied and Environmental Microbiology* 59 (3): 695–700. <https://doi.org/10.1128/aem.59.3.695-700.1993>.
- National Institute for Health and Care Excellence. 2016. "Healthcare-Associated Infections Quality Standard 113." Accessed June 07, 2024. <https://www.nice.org.uk/guidance/qs113>.
- Nurjadi, Dennis, Martin Scherrer, Uwe Frank, Nico T. Mutters, Alexandra Heinger, Isabel Späth, Vanessa M. Eichel, et al. 2021. "Genomic Investigation and Successful Containment of an Intermittent Common Source Outbreak of OXA-48-Producing *Enterobacter cloacae* Related to Hospital Shower Drains." *Microbiology Spectrum* 9 (3): e0138021-e0138021. <https://doi.org/10.1128/Spectrum.01380-21>.
- O'Neill, J. 2016. "Tackling Drug-Resistant Infections Globally: Final Report and Recommendations." The Review on Antimicrobial Resistance. [https://amr-review.org/sites/default/files/160518\\_Final%20paper\\_with%20cover.pdf](https://amr-review.org/sites/default/files/160518_Final%20paper_with%20cover.pdf)
- Parani, M., G. Lokhande, A. Singh, and A. K. Gaharwar. 2016. "Engineered Nanomaterials for Infection Control and Healing Acute and Chronic Wounds." *ACS Applied Materials & Interfaces* 8 (16): 10049–10069. <https://doi.org/10.1021/acsami.6b00291>.
- Park, S. C., H. Parikh, K. Vegesana, N. Stoesser, K. E. Barry, S. M. Kotay, S. Dudley, et al. 2020. "Risk Factors Associated with Carbapenemase-Producing Enterobacterales (CPE) Positivity in the Hospital Wastewater Environment." *Applied and Environmental Microbiology* 86 (24): e01715–01720. <https://doi.org/10.1128/AEM.01715-20>.
- Pearce, E. I., and D. G. Nelson. 1989. "Microstructural Features of Carious Human Enamel Imaged with Back-Scattered Electrons." *Journal of Dental Research* 68 (2): 113–118. <https://doi.org/10.1177/00220345890680020301>.
- Pirzadian, J., S. P. Hartevelde, S. N. Ramdutt, W. J. B. van Wamel, C. H. W. Klaassen, M. C. Vos, and J. A. Severin. 2020. "Novel Use of Culturomics to Identify the Microbiota in Hospital Sink Drains with and without Persistent VIM-Positive *Pseudomonas aeruginosa*." *Scientific Reports* 10 (1): 17052–17052. <https://doi.org/10.1038/s41598-020-73650-8>.
- Qayyum, S., and A. U. Khan. 2016. "Nanoparticles vs. Biofilms: A Battle against Another Paradigm of Antibiotic Resistance."

- MedChemComm* 7 (8): 1479–1498. <https://doi.org/10.1039/C6MD00124F>.
- Quick, J., N. Cumley, C. M. Wearn, M. Niebel, C. Constantinidou, C. M. Thomas, M. J. Pallen, et al. 2014. "Seeking the Source of *Pseudomonas aeruginosa* Infections in a Recently Opened Hospital: An Observational Study Using Whole-Genome Sequencing." *BMJ Open* 4 (11): e006278. <https://doi.org/10.1136/bmjopen-2014-006278>.
- Rashid, M. 2006. "A Decade of Adult Intensive Care Unit Design: A Study of the Physical Design Features of the Best-Practice Examples." *Critical Care Nursing Quarterly* 29 (4): 282–311. <https://doi.org/10.1097/00002727-200610000-00003>.
- Regev-Yochay, G., G. Smollan, I. Tal, N. Pinas Zade, Y. Haviv, V. Nudelman, O. Gal-Mor, et al. 2018. "Sink Traps as the Source of Transmission of OXA-48–Producing *Serratia marcescens* in an Intensive Care Unit." *Infection Control and Hospital Epidemiology* 39 (11): 1307–1315. <https://doi.org/10.1017/ice.2018.235>.
- Rummel, C. D., O. J. Lechtenfeld, R. Kallies, A. Benke, P. Herzsprung, R. Rynek, S. Wagner, A. Potthoff, A. Jahnke, and M. Schmitt-Jansen. 2021. "Conditioning Film and Early Biofilm Succession on Plastic Surfaces." *Environmental Science & Technology* 55 (16): 11006–11018. <https://doi.org/10.1021/acs.est.0c07875>.
- Salaie, R. N., A. Besinis, H. Le, C. Tredwin, and R. D. Handy. 2020. "The Biocompatibility of Silver and Nanohydroxyapatite Coatings on Titanium Dental Implants with Human Primary Osteoblast Cells." *Materials Science & Engineering. C, Materials for Biological Applications* 107: 110210. <https://doi.org/10.1016/j.msec.2019.110210>.
- Salonen, A., J. Nikkilä, J. Jalanka-Tuovinen, O. Immonen, M. Rajilić-Stojanović, R. A. Kekkonen, A. Palva, and W. M. de Vos. 2010. "Comparative Analysis of Fecal DNA Extraction Methods with Phylogenetic Microarray: effective Recovery of Bacterial and Archaeal DNA Using Mechanical Cell Lysis." *Journal of Microbiological Methods* 81 (2): 127–134. <https://doi.org/10.1016/j.mimet.2010.02.007>.
- Savage, V. J., I. Chopra, and A. J. O'Neill. 2013. "Staphylococcus aureus Biofilms Promote Horizontal Transfer of Antibiotic Resistance." *Antimicrobial Agents and Chemotherapy* 57 (4): 1968–1970. <https://doi.org/10.1128/aac.02008-12>.
- Schleifer, K.-H. 2004. "Microbial Diversity: Facts, Problems and Prospects." *Systematic and Applied Microbiology* 27 (1): 3–9. <https://doi.org/10.1078/0723-2020-00245>.
- Shi, Jingwen, Hanna L. Karlsson, Katarina Johansson, Vladimir Gogvadze, Lisong Xiao, Jiangtian Li, Terrance Burks, et al. 2012. "Microsomal Glutathione Transferase 1 Protects against Toxicity Induced by Silica Nanoparticles but Not by Zinc Oxide Nanoparticles." *ACS Nano* 6 (3): 1925–1938. <https://doi.org/10.1021/nn2021056>.
- Silverman, J. D., R. J. Bloom, S. Jiang, H. K. Durand, E. Dallow, S. Mukherjee, and L. A. David. 2021. "Measuring and Mitigating PCR Bias in Microbiota Datasets." *PLoS Computational Biology* 17 (7): e1009113. <https://doi.org/10.1371/journal.pcbi.1009113>.
- Singh, S., S. K. Singh, I. Chowdhury, and R. Singh. 2017. "Understanding the Mechanism of Bacterial Biofilms Resistance to Antimicrobial Agents." *The Open Microbiology Journal* 11 (1): 53–62. <https://doi.org/10.2174/1874285801711010053>.
- Stebounova, L. V., A. Adamcakova-Dodd, J. S. Kim, H. Park, P. T. O'Shaughnessy, V. H. Grassian, and P. S. Thorne. 2011. "Nanosilver Induces Minimal Lung Toxicity or Inflammation in a Subacute Murine Inhalation Model." *Particle and Fibre Toxicology* 8 (1): 5. <https://doi.org/10.1186/1743-8977-8-5>.
- Steinmetz, L., C. Geers, S. Balog, M. Bonmarin, L. Rodriguez-Lorenzo, P. Taladriz-Blanco, B. Rothen-Rutishauser, and A. Petri-Fink. 2020. "A Comparative Study of Silver Nanoparticle Dissolution under Physiological Conditions." *Nanoscale Advances* 2 (12): 5760–5768. <https://doi.org/10.1039/D0NA00733A>.
- Takahashi, S., J. Tomita, K. Nishioka, T. Hisada, and M. Nishijima. 2014. "Development of a Prokaryotic Universal Primer for Simultaneous Analysis of Bacteria and Archaea Using Next-Generation Sequencing." *PLoS One* 9 (8): e105592. <https://doi.org/10.1371/journal.pone.0105592>.
- Travnickova, E., P. Mikula, J. Oprsal, M. Bohacova, L. Kubac, D. Kimmer, J. Soukupova, and M. Bittner. 2019. "Resazurin Assay for Assessment of Antimicrobial Properties of Electrospun Nanofiber Filtration Membranes." *AMB Express* 9 (1): 183. <https://doi.org/10.1186/s13568-019-0909-z>.
- Vickery, K., A. Deva, A. Jacombs, J. Allan, P. Valente, and I. B. Gosbell. 2012. "Presence of Biofilm Containing Viable Multiresistant Organisms despite Terminal Cleaning on Clinical Surfaces in an Intensive Care Unit." *The Journal of Hospital Infection* 80 (1): 52–55. <https://doi.org/10.1016/j.jhin.2011.07.007>.
- Volling, Cheryl, Narges Ahangari, Jessica J. Bartoszko, Brenda L. Coleman, Felipe Garcia-Jeldes, Alaina J. Jamal, Jennie Johnstone, et al. 2020. "Are Sink Drainage Systems a Reservoir for Hospital-Acquired Gammaproteobacteria Colonization and Infection? A Systematic Review." *Open Forum Infectious Diseases* 8 (2): ofaa590. <https://doi.org/10.1093/ofid/ofaa590>.
- Walker, J. T., A. Jhutti, S. Parks, C. Willis, V. Copley, J. F. Turton, P. N. Hoffman, and A. M. Bennett. 2014. "Investigation of Healthcare-Acquired Infections Associated with *Pseudomonas aeruginosa* Biofilms in Taps in Neonatal Units in Northern Ireland." *The Journal of Hospital Infection* 86 (1): 16–23. <https://doi.org/10.1016/j.jhin.2013.10.003>.
- Withey, Z., T. Goodall, S. MacIntyre, and H. S. Gweon. 2021. "Characterization of Communal Sink Drain Communities of a University Campus." *Environmental DNA* 3 (5): 901–911. <https://doi.org/10.1002/edn3.196>.
- Wolf, I., P. W. Bergervoet, F. W. Sebens, H. L. van den Oever, P. H. Savelkoul, and W. C. van der Zwet. 2014. "The Sink as a Correctable Source of Extended-Spectrum Beta-Lactamase Contamination for Patients in the Intensive Care Unit." *The Journal of Hospital Infection* 87 (2): 126–130. <https://doi.org/10.1016/j.jhin.2014.02.013>.
- Xing, R., S. P. Lyngstadaas, J. E. Ellingsen, S. Taxt-Lamolle, and H. J. Haugen. 2015. "The Influence of Surface Nanoroughness, Texture and Chemistry of TiZr Implant Abutment on Oral Biofilm Accumulation." *Clinical Oral Implants Research* 26 (6): 649–656. <https://doi.org/10.1111/clr.12354>.
- Yang, B., Y. Wang, and P. Y. Qian. 2016. "Sensitivity and Correlation of Hypervariable Regions in 16S rRNA Genes in Phylogenetic Analysis." *BMC Bioinformatics* 17 (1): 135. <https://doi.org/10.1186/s12859-016-0992-y>.
- Yano, R., T. Shimoda, R. Watanabe, Y. Kuroki, T. Okubo, S. Nakamura, J. Matsuo, S. Yoshimura, and H. Yamaguchi. 2017. "Diversity Changes of Microbial Communities into Hospital Surface Environments." *Journal of Infection and Chemotherapy* 23 (7): 439–445. <https://doi.org/10.1016/j.jiac.2017.03.016>.
- Yu, Z., R. García-González, F. L. Schanbacher, and M. Morrison. 2008. "Evaluations of Different Hypervariable Regions of Archaeal 16S rRNA Genes in Profiling of Methanogens by

- Archaea-Specific PCR and Denaturing Gradient Gel Electrophoresis." *Applied and Environmental Microbiology* 74 (3): 889–893. <https://doi.org/10.1128/aem.00684-07>.
- Yui, S., M. Muzslay, K. Karia, B. Shuttleworth, S. Ali, N. Dudzinska, and P. Wilson. 2019. "Evaluation of Droplet Production by a New Design of Clinical Handwash Basin for the Healthcare Environment." *The Journal of Hospital Infection* 103 (1): e110–e114. <https://doi.org/10.1016/j.jhin.2019.06.014>.
- Zhou, Z., B. Hu, X. Gao, R. Bao, M. Chen, and H. Li. 2016. "Sources of Sporadic *Pseudomonas aeruginosa* Colonizations/Infections in Surgical ICUs: Association with Contaminated Sink Trap." *Journal of Infection and Chemotherapy* 22 (7): 450–455. <https://doi.org/10.1016/j.jiac.2016.03.016>.
- Zook, J. M., S. E. Long, D. Cleveland, C. L. Geronimo, and R. I. MacCuspie. 2011. "Measuring Silver Nanoparticle Dissolution in Complex Biological and Environmental Matrices Using UV-Visible Absorbance." *Analytical and Bioanalytical Chemistry* 401 (6): 1993–2002. <https://doi.org/10.1007/s00216-011-5266-y>.